CANADIAN THESES

THÈSES CANADIENNES

NOTICE

The quality of this microfiche is heavily dependent upon the quality of the original thesis submitted for microfilming. Every effort has been made to ensure the highest quality of reproduction possible.

If pages are missing, contact the university which granted the degree.

Some pages may have indistinct print especially if the original pages were typed with a poor typewriter ribbon or if the university sent us an inferior photocopy.

Previously copyrighted materials (journal articles, published tests, etc.) are not filmed.

Reproduction in full or in part of this film is governed by the Canadian Copyright Act, R.S.C. 1970, c. C-30. Please read the authorization forms which accompany this thesis.

AVIS

La qualité de cette microfiche dépend grandement de la qualité de la thèse soumise au microfilmage. Nous avons tout fait pour assurer une qualité supérieure de reproduction.

S'il manque des pages, veuillez communiquer avec l'université qui a conféré le grade.

La qualité d'impression de certaines pages peut laisser à désirer, surtout si les pages originales ont été dactylographiées à l'aide d'un ruban usé ou si l'université nous a fait parvenir une photocopie de qualité inférieure.

Les documents qui font déjà l'objet d'un droit d'auteur (articles de revue, examens publiés, etc.) ne sont pas microfilmés.

La reproduction, même partielle, de ce microfilm est soumise à la Loi canadienne sur le droit d'auteur, SRC 1970, c. C-30. Veuillez prendre connaissance des formules d'autorisation qui accompagnent cette thèse.

THIS DISSERTATION HAS BEEN MICROFILMED EXACTLY AS RECEIVED

LA THÈSE A ÉTÉ MICROFILMÉE TELLE QUE NOUS L'AVONS REÇUE

Canadä

/5)

0-315-26882-4

PERMISSION TO MICROFILM — AUTORISATION DE MICROFILMER

• Please print or type — Écrire en lettres moulées ou dactylographier

Full Name of Author — Nom complet de l'auteur

SHAHUL HAMEED NIHAR NILAR

Date of Birth — Date de naissance

14 MAR ...

Country of Birth — Lieu de naissance

SRI LANKA

Permanent Address — Résidence fixe

... DEHIWELA SRI LANKA

Title of Thesis — Titre de la thèse

A THEORETICAL SIMULATION OF INTERACTIONS IN

TRANSMEMBRANE IONIC CHANNELS

University — Université

THE UNIVERSITY OF ALBERTA, CANADA

Degree for which thesis was presented — Grade pour lequel cette thèse fut présentée

MASTER OF SCIENCE M.Sc.

Year this degree conferred — Année d'obtention de ce grade

1983

Name of Supervisor — Nom du directeur de thèse

DR. S. FRAGA.

Date

26 July 1983

Signature

NL-91 (4/77)

THE UNIVERSITY OF ALBERTA

A THEORETICAL SIMULATION OF INTERACTIONS IN

TRANSMEMBRANE IONIC CHANNELS

by

SHAHUL HAMEED MEERAN NILAR

Ⓒ

A THESIS

SUBMITTED TO THE FACULTY OF GRADUATE STUDIES AND RESEARCH

IN PARTIAL FULFILMENT OF THE REQUIREMENTS FOR THE DEGREE

OF MASTER OF SCIENCE

DEPARTMENT OF CHEMISTRY

EDMONTON, ALBERTA

FALL, 1983

THE UNIVERSITY OF ALBERTA

RELEASE FORM

NAME OF AUTHOR   Shahul Hameed Meeran Nilar

TITLE OF THESIS   A Theoretical Simulation of Interactions

in Transmembrane Ionic Channels

DEGREE FOR WHICH THESIS WAS PRESENTED   M.Sc.

YEAR THIS DEGREE GRANTED 1983

Permission is hereby granted to THE UNIVERSITY OF

ALBERTA LIBRARY to reproduce single copies of this

thesis and to lend or sell such copies for private,

scholarly or scientific research purposes only.

The author reserves other publication rights, and

neither the thesis nor extensive extracts from it may be

printed or otherwise reproduced without the author's

written permission.

(signed) _____

PERMANENT ADDRRESS:

3/8, Pinwatte Road

Dehiwela
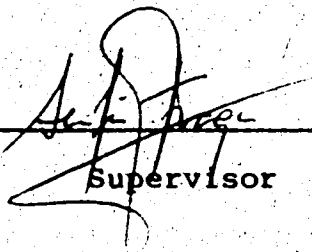
Sri Lanka

Dated 26 July   1983
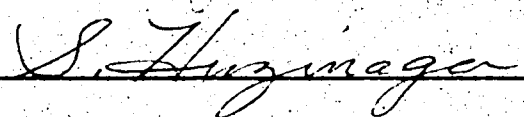
THE UNIVERSITY OF ALBERTA
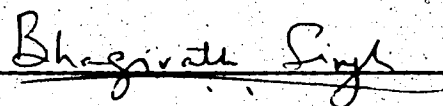
FACULTY OF GRADUATE STUDIES AND RESEARCH

The undersigned certify that they have read, and

recommend to the Faculty of Graduate Studies and Research,

for acceptance, a thesis entitled A THEORETICAL SIMULATION

OF INTERACTIONS IN TRANSMEMBRANE IONIC CHANNELS submitted by

SHAHUL HAMEED MEERAN NILAR in partial fulfilment of the

requirements for the degree of Master of Science.

_____
Supervisor

_____

_____

_____
External Examiner

Date 20 July , 1983

To my revered guru

DR. R. A. THURAISINGHAM

Department of Chemistry

University of Colombó

Sri Lanka

ABSTRACT

Reversible interference with the conductance properties of the Sodium channel by anesthetic molecules and preferred interaction with neurotransmitters in the synaptic cleft are two postulated mechanisms of general anesthesia.

In this thesis, both mechanisms have been studied and interaction energies used as the criterion to decide on the preferential binding of the model for the Sodium channel with ions and anesthetic molecules. The interaction energies were evaluated using a 1/R expansion parameterised to reproduce ab-initio energies.

Gramicidin-A dimer was chosen as a model for the Sodium channel and its structure generated by a theoretical conformation analysis. This model was refined in stages by simulating the lipid environment in the membrane with (i) formic acid molecules (ii) formic acid and octane molecules and (iii) formic acid, octane and a chain of water molecules through the channel.

At each stage of improvement of the model, the energy barriers and permeability ratios for the ions under consideration (Li^+, Na^+, K^+, Ca^{2+}) were evaluated and found to be consistent with the experimentally observed two-site binding theory.

The interaction of diethyl ether with the mouth of the channel was found to be preferred over that of a water molecule at the same position. Furthermore, the value of the energy of interaction is in the thermal range and the position of the ether is such as to block the mouth of the channel, thus interfering with the movement of the ions responsible for the depolarisation of the membrane. This hypothesis was tested on the guanidinium ion and the neurotoxins, tetrodotoxin and saxitoxin. Their toxicity is attributed to the large energy of interaction and complete blocking of the channel.

Interactions of diethyl ether with extracellular sodium ions, water and acetylcholine show a definite tendency for the favoured interaction of the ether with the neurotransmitter.

TABLE OF CONTENTS

LIST OF TABLES

Nervous transmission is the process by which cells in an organism communicate with each other and the basic cellular units responsible for the transfer of information are called neurons.

A neuron consists of a cell body which contains the cell nucleus. From the cell body, protrusions known as dendrites branch into the extracellular medium. In addition to the dendrites there is a long smooth extension of the cell body known as the axon at the end of which there are little fibres called terminal fibres. Insulation between the axons of two neurons is provided by another type of cell known as the Schwann cell. These cells are wrapped around the axon and the intercellular spaces along the length of the axon are called the nodes of Ranvier. Any branches from the axon occur at such nodal points.

Incoming information from another neuron, known as a signal, is received by the dendrites and conducted along the axon to other parts of the central nervous system (CNS). Communication between neurons is achieved by transmitting these signals across the gaps which separate the neurons. Such gaps are called synapses and, in the majority of the cases, a synapse separates the axon of one neuron from the

dendrite of another. The end of the axon enlarges at the synapse to form a terminal button which is associated with the transmittance of the signal across the synapse.

It has been observed experimentally (1-7) that in the resting state, the outside of an axon is more positive with respect to its interior and the associated potential difference is about -70 mV. A stimulus is required to change this state of the axon and when supplied in the form of an electric pulse causes a depolarisation, in the vicinity of the point of application, across the axonal membrane. This depolarisation, if in excess of a threshold value, has been found to overshoot with the consequent reversal of the polarity across the membrane. This impulse is called the action potential.

The resting state of the neuron is restored after a few milliseconds and the impulse travels along the axon due to the sequential depolarisation of its membrane. At the terminal button of the axon, the impulse is transmitted across the synapse resulting in the depolarisation of the membrane of a second neuron. In this manner, neurons transfer information to various parts of the CNS.

Communication across synapses could be in either of two forms:

(i) chemical transmission

(ii) electrical transmission

As little is known of electrical transmission, the emphasis

has been on chemical transmission which is described below. In this mode of communication, certain types of molecules are associated with the conduction of the signal across the synapse. The terminal button of an axon has spherical structures, known as synaptic vesicles, which contain these transmitter molecules. When an action potential arrives at the axonal terminal, some of the synaptic vesicles release the transmitters into the synaptic cleft. These molecules then diffuse across the synapse and interact with the dendrite membrane of a second neuron. Such interactions with the post-synaptic membrane causes a depolarisation on the second neuron and, therefore, the transmission of the impulse across the synapse.

In a neuron, the concentration of Na^+ in the external medium has been found to be about ten times greater than in the axoplasm, while the reverse holds true for K^+. Hodgkin et al (4-7) observed that the propagation of the nerve impulse corresponded to the change in the permeability of the axonal membrane to Na^+ and K^+.

The arrival of an impulse at a neuron allows the flow of Na^+ into the axoplasm with a simultaneous outflow of K^+. It is this transfer of ions which causes the depolarisation across the membrane. An immediate repolarisation process follows with the Na^+ being driven out of the axoplasm. This restores the neuron to its previous resting state. The restorative mechanism is called the

"Sodium pump" and the energy required to expel the Na^+ is supplied by the hydrolysis of Adenosine triphosphate (ATP). Thus the basic mechanism which causes an impulse and its propagation along the axon is directly associated with the permeability of the axonal membrane to ions.

The passage of an ion, unaided, through a lipid bilayer may not be energetically favourable due to the latter's hydrophobicity and a polar medium spanning the bilayer could help the ion migrate across the membrane. The polypeptide nature of integral membrane proteins satisfy these requirements and they behave as transmembrane channels that facilitate ionic migration. Such channels are selective towards certain ions and the Sodium channel, which allows the transport of Na^+ during nerve impulse, is a very relevant example.

Although the molecular weight of the Sodium channel has been found to be 270 kilo-daltons, its structure is still to be characterised. The average diameter of the channel pore is about 5 Å and conformational changes in the amino acid residues can vary this value according to the size of the ion being transported.

After initiating the pulse on the post-synaptic membrane, the transmitter molecules have no futher use and are destroyed by a related enzyme. After the molecules of the transmitter have been removed, a second impulse can be transmitted through the same intracellular gap.

The release of the neurotransmitter molecules into the synaptic cleft appears to be in small quantized amounts and their diffusion from the pre-synaptic to the post-synaptic membrane determines the direction of the action potential.

1.1 INHIBITORY EFFECTS ON NERVOUS TRANSMISSION

Interference with the initiation or propagation of a nerve impulse will result in the suppression of inter-neuronal communication. Such inhibitory effects could be permanent or temporary depending on the extent of the interference. Usually, molecules which interact with strategic biochemical components necessary for nervous transmission are associated with such effects, examples being neurotoxins and anesthetics.

The interference caused by anesthetics can be regarded as temporary and therefore reversible. That is, after a certain period of time, the inhibitory effect of the anesthetic is diminished and nervous transmission restored to normal levels. Hence the use of anesthetics in surgical applications. Neurotoxins on the other hand, have a more permanent inhibitory influence and in most cases the results are fatal (8).

Many mechanisms have been proposed (9) to explain the inhibitory effects on nervous transmission. Of these, the three that are currently emphasised are:

    (i)   interference with the initiation of the impulse

    (ii)   interactions which hinder the diffusion of the

transmitter molecules in the synaptic cleft

and

    (iii)   changes in the structure of the transmitter

receptor.

As the initiation of an impulse is directly linked with ionic transport through the Sodium channel, inhibition of nervous transmission may be due to the blocking of the channel by given molecules, thus hindering ionic migration. A logical point of hindrance is the pore of the channel and the interaction of the inhibitor molecules with the mouth of the pore could be one of the factors responsible for this interference.

Another possibility is the complexing of the inhibitor molecules with chemical transmitters like acetylcholine. The second hypothesis implies that such interactions should be more favourable than the corresponding interactions with other molecular and ionic species in the synaptic cleft. Further, the diffusion of a complexed transmitter towards the receptor on the post-synaptic membrane is hindered and thus, the probability of depolarising the second neuron significantly reduced.

Each neurotransmitter has its associated receptor on the post-synaptic membrane and interactions between the two which are responsible for the transmission of the impulse,

take place at strategic points on the receptor. The
blocking of such points by anesthetics or toxins diminishes
the transmitter-receptor interactions responsible for
nervous transmission. For example, the toxicity of curare
is believed to be due to the blocking of the active sites of
the receptor on the post-synaptic membrane.

The brief outlines of each of the three mechanisms
presented above give an indication of some of the possible
interactions responsible for the anesthetic or toxic
properties of some molecules. The reduction of inter-
neuronal communication may be due to any one or more of the
processes described by the postulated mechanisms. From a
chemical point of view, the third mechanism is more
difficult to investigate, as very little is known about the
receptor sites on the post-synaptic membrane. In the case
of the first two mechanisms the structural details of the
systems involved are better understood and can be
investigated by suitable simulations of the molecular
species and related environments.

1.2 AIM OF THIS RESEARCH

In this thesis an attempt has been made to understand
some of the possible molecular interactions which are
responsible for the inhibition of nervous transmission. The
first two of the three proposed mechanisms were studied

using theoretical simulation techniques. The energy of
interaction between two systems under investigation was used
as the criterion to decide on their preferential binding.
The mode of evaluation of this energy is described briefly
in the next subsection.

As the Sodium channel is not structurally fully
characterised, a suitable model based on available
experimental information was used instead. The energy
gradients for the passage of some alkali and alkali earth
ions through the model channel were determined and found to
be in good agreement with experiment. The toxicity of the
neurotoxins, tetrodotoxin and saxitoxin, was studied by
determining the nature of their interaction with the pore of
the channel. Further, the position of the toxins was found
to block the pore of the channel, interfering with the
transport of ions. This observation indicates that such
toxins hinder the depolarisation of the membrane and hence
nervous transmission.

A similar study on the anesthetic nature of diethyl
ether indicated that the energy of interaction of the ether
with the mouth of the pore was in the thermal range. Such
interactions are relatively weak and can be overcome by
molecular collisions and conformational changes in the
systems concerned - a prerequisite for the temporary
inhibition of nervous transmission as observed in
anesthesia.

The second postulated mechanism was studied next. Extracellular Na^+, acetylcholine and water were chosen as some of the species in the synaptic cleft. Molecules of diethyl ether were clustered around each of the species mentioned above. The interaction energy of each ether molecule with the second entity was evaluated. As postulated, the trend in these energies showed a definite preference for the interaction of the ether with acetylcholine than with Na^+ or water.

1.3 MODE OF EVALUATION OF INTERACTION ENERGIES

A quantum mechanical treatment of a system of interest requires the solution of the Schrodinger equation

$$H\psi = E\psi \qquad\qquad 1.2.1$$

where H is the Hamiltonian operator which includes all the interactions in the system, E and ψ being the corresponding eigenvalue and eigenfunction, respectively.

At present, exact solutions to this equation are available for hydrogen-like systems only and approximations are required for the treatment of larger systems. Most molecules involved in biochemical phenomena have many nuclei and electrons and the approximations invoked are, in many cases, drastic. The results obtained from such calculations

are questionable as the approximations and models used may

have very little relevance to the process under

investigation.

The Born-Oppenheimer approximation (10) which separates

the nuclear and electronic parts of the total wave function

ψ as

$$\psi = \psi_{electronic} \cdot \psi_{nuclear} \qquad 1.3.2$$

is a basis of most molecular electronic calculations.

Keeping the nuclear geometry fixed, the electronic energy of

the system and its approximate wave function can be

evaluated.

Ab-initio calculation of the electronic energy is

usually based on the Hartree-Fock-Roothan (11) self-

consistent field technique. The amount of computer time

required for such a treatment increases as a function of the

number of electrons to the fourth power. This has been the

main drawback in the rigorous application of this method to

large systems. The cost of such calculations will be

phenomenal in a meaningful treatment of biomolecules and to

overcome this disadvantage, semiempirical methods have been

used with varying degrees of success.

The method of calculation used in this thesis to

evaluate the interaction energy between two systems A and B

is based on the theory of weak interactions. An assumption

in this theory is that the wave functions of the constituent systems are not altered during interaction and therefore, a multipolar expansion of the potential of interaction is possible. Such a multipolar expansion expresses the interaction between A and B as a function of the reciprocal of the distance separating the various atoms and is referred to as a 1/R expansion.

The semiempirical method used here evaluates the interaction energy from a truncated 1/R expansion parameterised to reproduce ab-initio calculations. The details of the method of calculation are given in Chapter 2.

The reasons behind the choice of certain molecules for the simulation of the biological systems and environments and the results obtained from the application of the semiempirical formulation are presented in Chapter 3. Figures of the interacting systems are given to emphasise certain salient features of the results.

General conclusions on the applicability and improvements to the model are discussed in the final chapter.

CHAPTER 2 - THEORETICAL FORMULATION

2.1 INTRODUCTION

In order to evaluate the interaction energy between two systems A and B, a suitable potential energy function $V(r)$ has to be chosen. This function, which measures the interaction between A and B, will describe the difference in the total energy of the system at a distance r from its value when A and B are infinitely separated. Thus E_{total}, the total energy of the composite system, is given by

$$E_{total} = E_A + E_B + V(r) \qquad 2.1.1$$

where E_X (X = A, B) is the energy of the isolated system X. As the distance separating A and B increases, the influence of each system on the other decreases. Hence the values of $V(r)$ decreases with r and at infinite separation

$$E_{total} = E_A + E_B \qquad 2.1.2$$

$V(r)$ can be regarded as a cumulative effect of attractive and repulsive contributions between the particles constituting the systems. For chemical purposes, the particles are the electrons and protons of the atoms making

12

up A and B.

For theoretical purposes, the energy of interaction ΔE can be divided into

- (i) Long range contributions

(ii) Short range contributions.

At long range, the overlap of the wave functions is assumed to be small and thus the wave function ψ of the composite system can be expressed as a product $\psi_A \psi_B$ of the wave functions of the isolated systems (12-15). However, for interactions at short distances, such an assumption about the wave function of the total system is not valid as the overlap of the electron clouds is significant. In such a case, the total wave function is an antisymmetrised product of all the electrons in the composite system.

The long range contributions to ΔE can be subdivided into an electrostatic component $\Delta E_{electrostatic}$, an induction contribution ΔE_{ind} and a term ΔE_{disp} due to the dispersion energy. The physical meaning of each of these subdivisions is described below.

At a finite distance r separating A and B, the interaction of the charges on one system with that of the other introduces the electrostatic component $\Delta E_{electrostatic}$. The collection of charges on A induces a field on B, and vice-versa. The field induced by one system interacts with the other system and this component of ΔE is termed the induction energy ΔE_{ind}. The electron clouds in a

system are in continuous motion. Even if the interacting

systems have no permanent dipole moment, they will possess

an instantaneous dipole moment. The interaction between the

two instantaneous dipoles produces the dispersion energy

component, ΔE_{disp}, of ΔE.

Thus ΔE can be regarded as being composed of the

following contributions:

$$\Delta E = \Delta E_{electrostatic} + \Delta E_{ind} + \Delta E_{disp} + \Delta E_{short-range} \qquad 2.1.3$$

2.2 DERIVATION OF THE POTENTIAL ENERGY FUNCTION

2.2.1 ELECTROSTATIC CONTRIBUTIONS

The potential ϕ_P at a point P due to charges Q_1 and Q_2

arranged about a center of mass O is given by

$$\phi_P = \frac{1}{4\pi\varepsilon_0} \left[\frac{Q_1}{r_1} + \frac{Q_2}{r_2} \right] \qquad 2.2.1.1$$

where ε_0 is the permittivity in free space and r_1, r_2, the

distances of P from Q_1 and Q_2, respectively.

If θ is the positive angle $\overline{OP}$ makes with $\overline{Q_1Q_2}$ and z_1,

z_2 the distances of Q_1 and Q_2 from O,

$$\phi_P = \frac{1}{4\pi\epsilon_0}\left[\frac{Q_1}{[r^2+z_1^2+2rz_1\cos\theta]^{1/2}} + \frac{Q_2}{[r^2+z_2^2-2rz_2\cos\theta]^{1/2}}\right]$$

2.2.1.2

Assuming $r \gg z_1$, z_2 and expanding in powers of z_1/r and z_2/r using the binomial expansion,

$$\phi_P = \frac{1}{4\pi\epsilon_0}\left[\frac{Q_1+Q_2}{r} + \frac{(Q_2z_2-Q_1z_1)\cos\theta}{r^2}\right.$$

2.2.1.3

$$\left. + \frac{(Q_1z_1^2+Q_2z_2^2)}{2r^3}(3\cos^2\theta-1) + \ldots\right]$$

Substituting

$$Q = Q_1 + Q_2,$$

$$\mu = Q_2z_2 - Q_1z_1$$

and

$$H = Q_1z_1^2 + Q_2z_2^2$$

one obtains

$$\phi_P = \frac{1}{4\pi\epsilon_0}\left[\frac{Q}{r} + \frac{\mu\cos\theta}{r^2} + \frac{H}{2r^3}(3\cos^2\theta-1) + \ldots\right]$$ 2.2.1.4

Consider a second charge distribution (Q_1', Q_2') with centre of mass S. The relative orientation of (Q_1', Q_2') with respect to (Q_1, Q_2) is defined as follows:

(i) θ_1 and θ_2 are the angles made by OQ_1' and OQ_2' with OS repectively.

(ii) z_1 and z_2 are distances of Q_1' and Q_2' from S and

(iii) ϕ is the angle, measured in an anti-clockwise sense, made by (Q_1', Q_2') with (Q_1, Q_2) about the line OS.

The electrostatic component, $\Delta E_{electrostatic}$ of ΔE is given by

$$\Delta E_{electrostatic} = Q_1' \phi(r_1') + Q_2' \phi(r_2') \qquad 2.2.1.5$$

Using equation 2.2.1.4 and substituting

$$Q' = Q_1' + Q_2'$$
$$\mu' = Q_2' z_2' - Q_1' z_1'$$
$$H' = Q_2' z_2'^2 + Q_1' z_1'^2,$$

one obtains

$$\Delta E_{electrostatic} = \frac{1}{4\pi\varepsilon_0} [\frac{QQ'}{r} + \frac{1}{r^2} (Q'\mu\cos\theta_1 - Q\mu'\cos\theta_2) -$$

$$\frac{\mu\mu'}{r^3} (2\cos\theta_1\cos\theta_2 - \sin\theta_1\sin\theta_2\cos\phi) +$$

$$\frac{1}{2r^3} \{Q H' (3\cos^2\theta_2 - 1) + Q' H (3\cos^2\theta_1 - 1)\} + \dots]$$

$$2.2.1.6$$

2.2.2. INDUCTION ENERGY

Suppose E is the static electric field produced by system A and μ_{ind}, the induced dipole moment of system B due to E. Then, by definition,

$$\mu_{ind} = \alpha E \qquad\qquad 2.2.2.1$$

and

$$\Delta E_{ind} = -\int_0^E \alpha \varepsilon d\varepsilon$$

$$\qquad\qquad 2.2.2.2$$

$$= -\tfrac{1}{2}\alpha E^2$$

where α is the static polarisability of B.

The magnitude ε of the induced energy at P, at a distance r from O, is given by

$$\varepsilon = [(\frac{\partial\phi_P}{\partial r})^2 + \frac{1}{r}(\frac{\partial\phi_P}{\partial\theta})^2]^{\tfrac{1}{2}} \qquad\qquad 2.2.2.3$$

which becomes, taking into account equation 2.2.1.4,

$$\varepsilon = \frac{1}{4\pi\varepsilon_0}[\frac{Q^2}{r^4} + 4\mu\frac{Q\cos\theta_1}{r^5} + \frac{\mu^2}{r^6}(3\cos^2\theta_1+1)+\ldots]^{\tfrac{1}{2}} \qquad 2.2.2.4$$

Substituting equation 2.2.2.4 in 2.2.2.2, the induced energy, ΔE_{ind}, of the second system due to the field of the first one is

$$\Delta E_{ind} = -\frac{1}{2}\frac{\alpha'}{(4\pi\varepsilon_0)^2}\{\frac{Q^2}{r^4} + 4\mu\frac{Q\cos\theta_1}{r^5} + \frac{\mu^2}{r^6}(3\cos^2\theta_1+1) + \ldots\}$$

$$\qquad\qquad 2.2.2.5$$

where α' is the polarisability of the second system.

As in the case of electrostatic contributions, the total induced energy E_{ind}, when A and B interact is

$$\Delta E_{ind} = \frac{1}{(4\pi\epsilon_0)^2}[-\tfrac{1}{2}(\frac{\alpha' Q^2 + \alpha Q'^2)}{r^4} - 2(\frac{\mu Q \alpha' Cos\theta_1 + \mu' Q' \alpha Cos\theta_2)}{r^5}$$
$$-\frac{\{\mu^2\alpha'(3Cos^2\theta_1 + 1) + \mu'\alpha(3Cos^2\theta_2+1)\}-...]}{2r^6}$$

$$2.2.2.6$$

2.2.3   DISPERSION ENERGY

As stated in section 2.1, the dispersion energy component ΔE_{disp} of ΔE is due to the interaction of the instantaneous dipole moments of A and B. Thus, ΔE_{disp} will be given by

$$\Delta E_{disp} = \langle\psi|W_{dd}|\psi\rangle \qquad\qquad 2.2.3.1$$

where ψ is the wave function for the composite system and W_{dd}, the quantum mechanical operator for dipole-dipole interactions.

Expressing ψ as $\psi_A\psi_B$ (section 2.1), at long range separations, one has

$$\Delta E_{disp} = \langle\psi_A\psi_B|W_{dd}|\psi_A\psi_B\rangle \qquad\qquad 2.2.3.2$$

2.2.3.1 DERIVATION OF THE DIPOLE-DIPOLE INTERACTION
OPERATOR

The potential ϕ_i at a point P_i due to a charge e_i at Q_i is given by

$$\phi_i = \frac{e_i}{R_i} \qquad\qquad 2.2.3.1.1$$

where,

$$R_i = |r_i - r_Q| \qquad\qquad 2.2.3.1.2$$
$$r_i \equiv OP_i$$
$$r_Q \equiv OQ$$

with respect to an origin O. Expansion of ϕ_i using the Taylor-Maclaurin expansion yields

$$\phi_i = \frac{e_i}{r_i} + e_i \sum_j^3 x_{Q,j} \left[\frac{\partial}{\partial x_{Q,j}} \left(\frac{1}{R_i} \right) \right]_{R_i = r_i} +$$

$$\frac{1}{2} q_i \sum_{j,k}^3 x_{Q,j} x_{Q,k} \left[\frac{\partial^2}{\partial x_{Q,k} \partial x_{Q,j}} \left(\frac{1}{R_i} \right) \right]_{R_i = r_i} + \qquad\qquad 2.2.3.1.3$$

Differentiating equation 2.2.3.1.2 with respect to the Cartesian components, yields

$$\frac{\partial f_{(R_i)}}{\partial x_{Q,j}} = - \frac{\partial f_{(R_i)}}{\partial x_{P,j}} \qquad\qquad 2.2.3.1.4$$

and substituting equation 2.2.3.1.4 in equation 2.2.3.1.3, the dipole potential $\phi^{(2)}$ due to N charged particles becomes

$$\phi^{(2)} = \sum_{i=1}^{N} e_i \sum x_{Q,j} \frac{\partial}{\partial x_{p,j}} \left(\frac{1}{r}\right)$$

$$= - p \cdot \nabla \left(\frac{1}{r}\right) \qquad\qquad 2.2.3.1.5$$

$$= \frac{p \cdot r}{r^3}$$

where p is the dipole moment of the system, defined as

$$p = \sum_{i=1}^{N} e_i \sum_{j=1}^{3} x_{Q,j} \qquad\qquad 2.2.3.1.6$$

The electric dipole field vector $E^{(2)}$ is given by

$$E^{(2)} = - \nabla \phi^{(2)}$$

$$= -\nabla \frac{(p \cdot r)}{r^3}$$

$$= - \frac{1}{r^3} \nabla(p \cdot r) - (p \cdot r) \nabla\left(\frac{1}{r^3}\right)$$

$$= - \frac{p}{r^3} + (p \cdot r) \frac{3r}{r^5}$$

$$= \frac{1}{r^5} [3(p \cdot r)r - pr^2] \qquad\qquad 2.2.3.1.7$$

If the interacting systems A and B, have dipoles p_A and p_B such that

$$p_A = er_A \qquad\qquad 2.2.3.1.8$$

and

$$p_B = er_B \qquad\qquad\qquad 2.2.3.1.9$$

where r_X (X = A, B) is the distance of the electron cloud from nucleus X, the dipole-dipole interaction energy E_{dd} is then given by

$$E_{dd} = \frac{e^2}{r^3} [r_A \bullet r_B - 3(r_A \bullet n)(r_B \bullet n)] \qquad 2.2.3.1.10$$

where n is the unit vector in the direction $\overline{AB}$.

The dipole-dipole interaction operator W_{dd} is then

$$W_{dd} = \frac{e^2}{r^3} [x_A x_B + y_A y_B - 2z_A z_B] \qquad 2.2.3.1.11$$

2.2.3.2   PERTURBATION FORMULATION OF THE DISPERSION

            ENERGY.

The first and second order perturbation changes to the energy of the systems A and B, $E_0^{(1)}$ and $E_0^{(2)}$ are given by

$$E_0^{(1)} = \langle \psi_A \psi_B | W_{dd} | \psi_A \psi_B \rangle \qquad 2.2.3.2.1$$

and

$$E_0^{(2)} = - \sum_v \sum_u \frac{|<\psi_A \psi_B |W_{dd}| \psi_{A_u} \psi_{B_v}>|^2}{E_{A_u B_v} - E_{AB}} \qquad 2.2.3.2.2$$

where E_{AB} is the total energy of the isolated systems A and B obtained by separate solution of their Schrodinger equations and $E_{A_u B_v}$ is the sum of the energies of A and B in the states u and v.

The dispersion contribution to the energy, correct to second order, is:

$$\Delta E_{disp} = E_0^{(1)} + E_0^{(2)} \qquad 2.2.3.2.3$$

Assuming that ψ is spherically symmetric, $E_0^{(1)} = 0$ from equations 2.2.3.2.1 and 2.2.3.1.11 one obtains

$$\Delta E_{disp} = E_0^{(2)} \qquad 2.2.3.2.4$$

From equations 2.2.3.1.11 and 2.2.3.2.2

$$\Delta E_{disp} = -\frac{e^2}{r^6} \sum_u \sum_v \{<\psi_A|x_A|\psi_{A_u}><\psi_B|x_B|\psi_{B_v}>$$
$$+ <\psi_A|y_A|\psi_{A_u}><\psi_B|y_B|\psi_{B_v}> \qquad 2.2.3.2.5$$
$$-2<\psi_A|z_A|\psi_{A_u}><\psi_B|z_B|\psi_{B_v}>\}^2 / [E_{A_u B_v} - E_{AB}]$$

Inclusion of dipole-quadrupole interactions and quadrupole-quadrupole interactions will include higher order terms in r.

In general, the dispersion energy, ΔE_{disp} can be expressed as

$$E_{disp} = \frac{C_6}{r^6} + \frac{C_8}{r^8} + \frac{C_{10}}{r^{10}} + \ldots \qquad 2.2.3.2.6$$

where, in particular, C_6/r^6 is given by equation 2.2.3.2.5.

2.2.4   SHORT RANGE CONTRIBUTIONS

In the short range region, there is considerable overlap of the wave-functions of the two systems A and B. Hence, the perturbation treatment as presented in 2.2.3 and the multipolar expansions used to derive the long range contributions are not strictly valid.

In order to overcome these difficulties, an empirical potential form is used to represent these short range forces. The functional form used generally is the Lennard-Jones (6-12) (16) given as

$$\Delta E_{short-range} = \varepsilon \left\{ \left(\frac{r_n}{r}\right)^{12} - 2\left(\frac{r_n}{r}\right)^6 \right\} \qquad 2.2.4.1$$

where r_n and ε are the equilibrium distance for the pair-potential interaction and ε, the depth of the potential energy minimum with respect to the energy of the systems at infinite separation.

2.2.5   SUMMARY OF THE ANALYTICAL FORMULATION FOR THE

INTERSYSTEM POTENTIAL ENERGY

From subsections 2.2.1 - 2.2.4, the interaction energy ΔE can be expressed as:

$$\Delta E = \frac{A_1}{R} + \frac{A_2}{R^2} + \frac{A_3}{R^3} + \frac{A_4}{R^4} + \frac{A_6}{R^6} + \frac{A_8}{R^8} + \frac{A_{10}}{R^{10}} + \frac{A_{12}}{R^{12}} + \ldots \quad 2.2.5.1$$

where the A_i's are coefficients associated with the corresponding powers of R.

For practical applications, such an equation is of little use and a semiempirical evaluation of some of the coefficients and suitable truncation of the multipolar expansion is required.

2.2.6   A SEMI-EMPIRICAL APPROACH TO THE R^6 COEFFICIENT

OF THE DISPERSION CONTRIBUTION - THE SLATER-

KIRKWOOD FORMULA[17]

The dispersion contribution, ΔE_{disp}, to the interaction between spherically symmetric atoms (see equation 2.2.3.2.5) may be written (in atomic units) as

$$\Delta E_{disp} = -\frac{6}{r^6} \sum_u \sum_v \frac{\langle \psi_A | z_A | \psi_{A_u} \rangle^2 \langle \psi_B | z_B | \psi_{B_v} \rangle^2}{(E_{A_u} E_{B_v} - E_{AB})} \quad 2.2.6.1$$

$$= -\frac{6}{r^6} \sum_u \sum_v \left(\frac{z_{A_u}^2 \, z_{B_v}^2}{(E_A(u,0) + E_B(v,0))} \right) \qquad 2.2.6.2$$

with

$$z_{A_u} = \langle \psi_A | z_A | \psi_{A_u} \rangle$$

$$z_{B_v} = \langle \psi_B | z_B | \psi_{B_v} \rangle$$

$$E_{A_u B_v} - E_{AB} = E_{A_u} + E_{B_v} - E_A - E_B = E_A(u,0) + E_B(v,0)$$

$$2.2.6.3$$

where $E_X(m,0)$ represents the energy of atom X in state m referred to the energy of its ground state (X = A, B; m = u,v).

A simplification of this expression may be achieved, as discussed below, through its relationship to the integral

$$I = \int_{-\infty}^{\infty} \frac{E_A(u,0) \, z_{A_u}^2 E_B(v,0) z_{B_v}^2}{(E_A(u,0)^2 + t^2)(E_B(v,0)^2 + t^2)} \, dt \qquad 2.2.6.4$$

The integral I can be expressed as

$$I = \lim_{R \to \infty} \int_{-R}^{R} \frac{E_A(u,0) \, z_{A_u}^2 \, E_B(v,0) \, z_{B_v}^2}{(E_A(u,0)^2 + t^2)(E_B(v,0)^2 + t^2)} \, dt$$

$$2.2.6.5$$

$$+ \int_{\Gamma} \frac{E_A(u,0) \, z_{A_u}^2 \, E_B(v,0) \, z_{B_v}^2}{(E_A(u,0)^2 + t^2)(E_B(v,0)^2 + t^2)} \, dt$$

where Γ is a semicircle above the x axis having the line $(-R, +R)$ as diameter. In the limit as $R \to \infty$, the second

term in equation 2.2.6.5 vanishes and, using the theorem of
residues, one obtains

$$I = \frac{\pi \, z_{A_u}^2 \, z_{B_v}^2}{(E_A(u,0) + E_B(v,0))} \qquad \qquad 2.2.6.6$$

Comparing equations 2.2.6.4 and 2.2.6.6 with equation
2.2.6.2 one obtains

$$\Delta E_{disp} = \frac{-6}{\pi r^6} \sum_u \sum_v \int_{-\infty}^{\infty} \frac{E_A(u,0)E_B(v,0)z_{A_u}^2 z_{B_v}^2}{(E_A(u,0)+t^2)(E_B(v,0)+t^2)} \, dt$$

$$2.2.6.7$$

Making use of the formula for the frequency dependent
polarisability $P(\nu)$ of an atom (18), namely

$$P(\nu) = 2 \sum_u \frac{E_A(u,0) \, z_{A_u}^2}{(E_A(u,0)-(h\nu)^2)}$$

and introducing an imaginary frequency $s = ih\nu$, the above
equation can be written as

$$P(s) = 2 \sum_u \frac{E_A(u,0) \, z_{A_u}^2}{(E_A(u,0) + s^2)} \qquad \qquad 2.2.6.8$$

Substitution of equation 2.2.6.8 in 2.2.6.7 yields

$$\Delta E_{disp} = \frac{-3}{\pi r^6} \int_0^{\infty} P_A(s) \, P_B(s) \, ds \qquad \qquad 2.2.6.9$$

The analytical expression of Mavroyannis et al (19)
expresses $P_A(s)$ as

$$P_A(s) = \frac{D^2}{d^2 + s^2} \qquad\qquad 2.2.6.10$$

The constants D and d are adjusted so as to reproduce the
static polarisability α as

$$\frac{D}{d^2} = \alpha \qquad\qquad 2.2.6.11$$

and the polarisability at large frequencies as

$$D = \frac{\sum\limits_w f_{0w}}{4\pi^2} \qquad\qquad 2.2.6.12$$

where f_{0w} is the oscillator strength for the transition from
the state 0 to state w.

Using the Thomas-Reiche-Kuhn rule, which equates the
total oscillator strength to the total number of electrons
on atom A, and equations 2.2.6.11 and 2.2.6.12, the
dispersion energy component of the interaction energy can be
written as

$$\Delta E_{disp} = \frac{3}{\pi r^6} \int\limits_0^\infty \frac{D_A D_B}{(d_A^2 + s^2)(d_B^2 + s^2)}\, ds \qquad\qquad 2.2.6.13$$

After evaluating the integral in the above equation, one
obtains

$$\Delta E_{disp} = \frac{-3}{2r^6} \frac{\alpha_A \alpha_B}{[(\frac{\alpha_A}{N_A})^{1/2} + (\frac{\alpha_B}{N_B})^{1/2}]} \qquad 2.2.6.14$$

Equation 2.2.6.14 is referred to as the Slater-Kirkwood formula for the dispersion energy contribution.

2.3.   APPLICATION OF THE 1/R EXPANSION

The 1/R expansion has been applied in the evaluation of interaction energies for

(i)   Intramolecular interactions

and

(ii)   Intermolecular interactions

2.3.1 INTRAMOLECULAR INTERACTIONS

In the method of Scheraga et al (20-24), the conformational energy of a polypeptide chain is considered as a function of the various dihedral angles and evaluated as a sum of the leading terms of the coulombic, dispersion and repulsion contributions derived in the foregoing subsections. A torsional energy contribution for rotations about dihedral angles and a semiempirically fitted hydrogen-bonding energy term are also included. A result of this formulation was the estimation of parameters to be used in empirical potential energy functions for pair-wise additive interactions.

The coulombic term E^C is given by

$$E^C = \sum_i \sum_j q_i q_j / D r_{ij} \qquad\qquad 2.3.1.1$$

where q_k is the electronic charge on atom k calculated by
the complete neglect of differential overlap method (25), D
is an effective dielectric constant given a value 2 and r_{ij},
the distance between atoms i and j.

The repulsion and dispersion energy terms, together
called the non-bonding term, are evaluated using a Lennard-
Jones (16) function as

$$E_{Non-bonded} = \sum_i \sum_j (A_{k\ell}/r_{ij}^{12} - C_{k\ell}/r_{ij}^{6}) \qquad\qquad 2.3.1.2$$

where $C_{k\ell}$ is obtained using the Slater-Kirkwood formula
(2.2.6.14).

The Lennard-Jones formula for the interaction between
two similar atoms k gives A_{kk} as

$$A_{kk} = -\epsilon^{kk} \langle r_g^{kk} \rangle^{12} \qquad\qquad 2.3.1.3$$

with r_g^{kk} and ϵ defined in section 2.2.4. The brackets
enclosing r_g^{kk} denote an average value, i.e.,

$$\langle r_g^{k\ell} \rangle = (\langle r_g^{kk} \rangle + \langle r_g^{\ell\ell} \rangle)/2 \qquad\qquad 2.3.1.5$$

with

$$\varepsilon_{k\ell} = -C^{k\ell}/2\langle r_g^{k\ell}\rangle^6 \qquad 2.3.1.6$$

one obtains

$$A^{k\ell} = -\varepsilon^{k\ell}\langle r_g^{k\ell}\rangle^{12} \qquad 2.3.1.7$$

The hydrogen bonding contributions E_{HB} are given (21) by:

$$E_{HB} = \sum_k \sum_\ell (A'_{H...X}/r_{H...X}^{12} - B'_{H...X}/r_{H...X}^{10}) \qquad 2.3.1.8$$

where the summation includes only the hydrogen-bonded pairs. The constants $A'_{H...X}$ and $B'_{H...X}$ are evaluated (21) by fitting the hydrogen bonding contribution of linear bonded dimers evaluated by the complete neglect of differential overlap method to a $(R^{-10} + R^{-12})$ expansion.

For rotations about a peptide bond, the torsional energy term (in kJ/mole) is evaluated using:

$$E_{tor} = (\frac{4.828}{2}) (1-Cos2\theta) \qquad 2.3.1.9$$

where θ is the torsional angle, while E_{tor} for rotations of the side chain dihedral angles (x) is given by:

$$E_{tor} = (U_0/2)(1 \pm \text{Cos } 3x) \qquad\qquad 2.3.1.10$$

---

where

U_0

$\equiv 0.6453$ kJ/mole for rotations about C-C saturated bonds

$\equiv 0.1434$ kJ/mole for rotations about C-O hydroxyl bonds

$\equiv 0.4302$ kJ/mole for rotations about C-N amine bonds

2.3.2 INTERMOLECULAR INTERACTIONS

From section 2.2.5, the energy of interaction ΔE_{AB} between two molecules A and B can be evaluated as a sum of individual interatomic pair potentials according to the equation

$$\Delta E_{AB} = \sum_{a \in A} \sum_{b \in B} \left[\frac{A_{ab}}{R_{ab}} + \frac{B_{ab}}{R_{ab}^2} + \frac{C_{ab}}{R_{ab}^3} + \ldots \right] \qquad 2.3.2.1$$

where A_{ab}, B_{ab}, C_{ab}, can be obtained by comparison with equations 2.2.1.6, 2.2.2.6, 2.2.4.1 and 2.2.6.14. The form of equation 2.2.5.1 makes its practical applicability and usefulness questionable. For computational purposes, the first term in each of the contributions to ΔE_{AB} are used to evaluate the energy of interaction.

A particular example is the potential energy function of Minicozzi and Bradley (26) which approximates ΔE_{AB} as:

$$\Delta E_{AB} = \sum_{a \in A} \sum_{b \in B} \left(\frac{A_{ab}}{R_{ab}} + \frac{B_{ab}}{R_{ab}^4} + \frac{C_{ab}}{R_{ab}^6} + \frac{D_{ab}}{R_{ab}^{12}} \right) \qquad 2.3.2.2$$

where

$$A_{ab} \equiv Q_a Q_b \qquad\qquad 2.3.2.3$$

$$B_{ab} \equiv - \tfrac{1}{2} (\alpha_a Q_b^2 + \alpha_b Q_a^2) \qquad\qquad 2.3.2.4$$

$$C_{ab} \equiv - 3/2 \; \alpha_a \alpha_b \left[\left(\frac{\alpha_a}{n_a}\right)^{1/2} + \left(\frac{\alpha_b}{n_b}\right)^{1/2} \right] \qquad 2.3.2.5$$

$$D_{ab} \equiv D_a D_b \qquad (27)$$

Q_x, α_x, r_x and D_x are, respectively, the electronic charge, static polarisability, effective number of electrons and a semiempirical parameter associated with atom X.

Another example of a 1/R expansion is that reported by Clementi et al (28-30) which expresses the interaction energy ΔE_{AB} as

$$\Delta E_{AB} = \sum_{a \in A} \sum_{b \in B} \left(\frac{A_{ab}}{R_{ab}} + \frac{B_{ab}}{R_{ab}^6} + \frac{C_{ab}}{R_{ab}^{12}} \right) \qquad 2.3.2.6$$

The above equation breaks down the interaction energy into pairwise contributions and the constants A_{ab}, B_{ab} and C_{ab} are evaluated by fitting the interaction energy between two systems A and B calculated in the self-consistent field (SCF) approximation to equation 2.3.2.6. A disadvantage in a formulation of this type is that each atom pair a,b has a set of constants (A_{ab}, B_{ab}, C_{ab}) associated with it. Many

such sets have to be evaluated for the interaction of large molecules. This reduces the practical applicability of the scheme.

In order to overcome this drawback, an atom in a molecule is assigned to classes based on its net atomic charge and molecular orbital valence state (MOVS) (31). The MOVS represent the one-center contributions to the SCF energy and reflect the environment of the atoms in a molecule.

In references (28-30), the interaction energy for each of the twenty-six amino acids with water have been calculated. The water molecule was placed at different positions so as to describe the interaction between the two systems as completely as possible.

The atoms in each amino acid are assigned to their classes and the constants (A, B, C) evaluated for the interactions of the atoms in each class with the hydrogen and oxygen of water.

2.4 METHOD OF CALCULATION

In this thesis, the potential energy function of Minicozzi and Bradley (26), modified at the R^4 and R^6 terms was used to evaluate the interaction energy between two systems A and B. The expression used for the calculation of ΔE_{AB} was:

$$\Delta E_{AB} = \sum_{a \varepsilon A} \sum_{b \varepsilon B} \{ \frac{Q_a Q_b}{R_{ab}} - \frac{1}{2} (\frac{f_a \alpha_a Q_b^2 + f_b \alpha_b Q_b^2}{R_{ab}^4})$$

$$- \frac{3}{2} f_a f_b \alpha_a \alpha_b / [(\frac{f_a \alpha_a}{n_a})^{1/2} + (\frac{f_b \alpha_b}{n_b})^{1/2}] R_{ab}^6 \qquad 2.4.1$$

$$+ \frac{g_a g_b}{R_{ab}^{12}} \}$$

or

$$\Delta E_{AB}(kJ/mole) = \sum_{a' \varepsilon A} \sum_{b' \varepsilon B} \{ 0.13894168 \times 10^4 \ Q_a Q_b / R_{ab}$$

$$- 0.69470838 \times 10^3 \ (f_a \alpha_a Q_b^2 + f_b \alpha_b Q_a^2) / R_{ab}^4$$

$$- 0.15160732 \times 10^4 \ f_a f_b \alpha_a \alpha_b / [(f_a \alpha_a / n_a)^{1/2}$$

$$+ (f_b \alpha_b / n_b)^{1/2}] R_{ab}^6 + 4.184 \frac{g_a g_b}{R_{ab}^{12}} \} \qquad 2.4.2$$

f_X, g_X are parameters associated with class X, with the summation now extending over the classes.

The interaction energy between atoms belonging to a particular class obtained from the expression of Clementi et al (28-30) was equated to equation 2.4.2. For values of the interatomic separation, starting at 2 Å with increments of 0.25 Å, the interaction energy calculated from equation 2.3.2.6 was fitted to equation 2.4.2. The f factor was assigned an initial value of 0.1 with increments of 0.1, and the best fit between the two expressions gives the g and

corresponding f factor (32,33) associated with the atom belonging to a particular class.

For the interactions between an ion and atoms of a certain class, the coefficients A_{ab}, B_{ab} and C_{ab} as reported (28-30) are not valid. This is mainly due to the fact that the type and magnitude of the interactions involved are different from that between two neutral molecules. Therefore, when an ion interacts with an atom, a new set of f and g factors consistent with this type of interaction have to be evaluated.

Ab-initio calculations for the interaction of Na^+ with ether, thioether and amide systems have been reported (34). Using the pair potential constants, A_{ab}, B_{ab} and C_{ab}, reported for these interactions, atoms were assigned to additional classes. The f and g factors corresponding to the new classes were calculated as described in the foregoing paragraphs.

Table 1 gives the class number and a brief description of the environment of the atom. The f and g factors along with the polarisabilities and net charge are given in Table 2

A major aim of this research was the evaluation of energy gradients for ions such as Li^+, Na^+, K^+ and Ca^{2+} during their movement through transmembrane channels. As such, it was necessary to calculate the corresponding parameters for the ions mentioned.

TABLE 1 - ASSIGNMENT OF ADDITIONAL CLASSES TO ATOMS

ATOM	CLASS	DESCRIPTION OF ATOMIC ENVIRONMENT
C	38	adjacent to $-CH_2-O$
C	41	CH_2, adjacent to ether O
C	42	C of $C{=}O$, OH (carboxylic acid carbon)
N	43	amide N
O	44	ether O
O	45	carboxylic O
H	48	CH_3, adjacent to $C{=}O$, N
H	49	CH_3, adjacent to CH_2
H	50	CH_3, adjacent to amide N
H	53	$-CH_2$
H	56	$-CH_2$, adjacent to ether O
H	57	-amino H

TABLE 2 - PARAMETERS FOR THE NEW CLASSES OF ATOMS

ATOM	CLASS	NET CHARGE	POLARIS-ABILITY (A^3)	f	g (kcal $^{1/2}$ A^6 mol $^{-1/2}$)
C	38	-.584	3.20	0.1	1492
	41	-.151	2.03	0.1	1093
	42	.421	1.30	14.2	1098
N	43	-.328	1.56	0.1	530
O	44	-.407	1.20	0.1	656
	45	-.406	1.18	0.1	655
H	48	.203	.362	27.2	561
	49	.187	.368	22.5	425
	50	.194	.365	23.4	456
	53	.195	.365	23.6	442
	56	.170	.376	19.9	383
	57	.266	.330	32.6	625

The energies of the systems $(X-X)^{n+}$, where $X = Li$, Na, K, $n = 2$; $X = Ca$, $n = 4$, were calculated as a function of the interionic distances using a standard self-consistent field technique. The basis sets used for the alkali ions were those reported in the literature (35-36). For Ca^{2+}, a basis set was generated as described below. The basis set for K^+ (34) was scaled to the atomic charge of Calcium. With this set as the initial guess, the 17s and 11p primitive basis functions were optimised within the SCF approximation.

The method of Huzinaga et al (37) was used to generate a d polarisation function for the optimised primitive basis set. The energy of Ca^{2+} using the (17s/11p/1d)* basis set (the asterix * denotes the inclusion of the d function) was evaluated. As the interaction energy for the dicationic system was required, it was decided to contract the primitive basis set to a (9s/6p/1d)* basis to reduce the computation involved.

Table 3 gives the basis set for Ca^{2+} and the energies for the different sets considered are listed in Table 4. The parantheses in column 5 of Table 3 show the order of contraction of the (17s/11p/1d)* basis.

TABLE 3 - BASIS SET FOR Ca^{2+}

FUNCTION NO.	TYPE	ORBITAL EXPONENT	COEFFICIENT	CONTRACTED FUNCTION NO.
1	s	616081.40	0.0003989	
2	s	91024.189	0.0031309	
3	s	19819.286	0.0168379	1
4	s	5486.6766	0.0745908	
5	s	1806.0119	0.2587144	
6	s	661.37163	0.72177445	
7	s	263.20103	0.38624719	
				2
8	s	113.46395	0.64339195	
9	s	50.064998	0.78925512	
				3
10	s	21.006017	0.23416483	
11	s	9.441946	1.0	4
12	s	4.2428535	1.0	5
13	s	1.6680995	1.0	6
14	s	0.990167	1.0	7
15	s	0.64233295	1.0	8
16	s	0.33077521	0.99741795	
				9
17	s	0.0408167	0.005200197	
18	p	1635.0249	0.005112976	
19	p	358.18464	0.042569083	10
20	p	108.44291	0.22425999	
21	p	38.424956	0.80820775	
22	p	15.249925	0.48396169	
				11
23	p	6.5276260	0.56868506	
24	p	2.9077000	1.0	12
25	p	1.4962640	1.0	13
26	p	0.7307220	1.0	14
27	p	0.3547250	0.93958945	
				15
28	p	0.1695930	0.070519148	
29	d*	1.047	1.0	16

TABLE 4 - BASIS SETS AND THEIR ENERGIES

BASIS SET	ENERGY (a.u.)
(17s/11p)	-676.151749
(17s/11p/1d)*	-676.151753
(9s/6p/1d)*	-676.133512
(contracted)	
Hartree-Fock value (38)	-676.1544

Interaction energies ΔE, as a function of the distance R, for the di-ionic systems were defined as:

$$\Delta E_{(R)} = E_{X_2^{n+}(R)} - E_{X_2^{n+}(L)} \qquad \qquad 2.4.3$$

The contracted basis set was then used to calculate the energy of Ca^{2+}-Ca^{2+} for different interionic distances. where L denotes a very large inter-ionic distance, the value of which depends on the system under consideration. This definition was used so as to reduce any basis set superposition errors (39-40).

The interaction energies obtained from equation 2.4.3
are fitted to equation 2.4.2 and the corresponding
parameters obtained for the best fit.

Table 5 gives the ions and their corresponding
parameters.

TABLE 5 - f AND g FACTORS FOR THE IONS

ION	CLASS	f	g
			$(kcal^{1/2} A^6 mol^{-1/2})$
Li^+	58	11.4	37
Na^+	59	5.1	563
K^+	60	1.0	1415
Ca^{2+}	61	1.6	8644

2.5 PROGRAMMING DETAILS

The FORTRAN program used for the evaluation of the interaction energy of two systems (41) uses a Steepest-Descent method for the minimum energy search.

2.5.1 STEEPEST-DESCENT METHOD

A steepest-descent procedure of minimisation of a function F requires

(i)   the selection of a starting point x_0

(ii)   evaluation of the gradient vector $G(0)$ of F at x_0

(iii)   minimising the function $f = F(x_0 - \lambda G_0)$, where λ is a variable step length corresponding to the largest decrease in the value of the function.

If the minimum within the desired level of convergence is not obtained, x_0 is varied as:

$$x_0 = x_0 - \lambda G_0$$
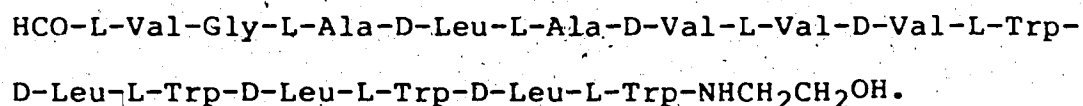
and the process repeated from step (2) above.

In the case of large systems, specially biomolecules,
the potential energy contour could be composed of multiple
minima. The result obtained by a steepest-descent technique
could then correspond to a minimum of the contour, which may
not be the global minimum.

CHAPTER 3 - RESULTS OF THE CALCULATIONS

The intracellular medium of a neuron has a higher concentration of K^+ compared to its exterior, while Na^+ are found in larger concentrations outside the cell. As discussed in Chapter 1, the transport of these ions through the Sodium channel and the consequent changes in the ratio of their intracellular to extracellular concentrations is responsible for the action potential. This action potential, propagated along the nerve axon, is primarily responsible for the release of the neurotransmitters into the synaptic cleft. Thus, the permeability of the Sodium channel to ions is important in understanding the mechanisms of nervous transmission.

As the structure of the Sodium channel is still to be elucidated, suitable models have to be used in order to study its interactions with ions. The choice of the model is based on the experimental information available. It has been found (42) that ions having a diameter larger than 5 Å hardly penetrate the channel and, furthermore, that a decrease in the pH significantly reduces the conductance of the ions through the channel. The latter observation suggests that in its active form the Sodium channel has negatively charged carboxylate groups. These groups can then be thought of as an effective coordination sphere which facilitates the passage of the cations.

Antibiotics synthesised by microorganisms make
membranes permeable to certain ions. The linear polypeptide
Gramicidin-A is an example of such a transmembrane
antibiotic which specifically facilitates the diffusion of
monovalent cations (43-46). It consists of fifteen amino
acid residues arranged in the following sequence:

HCO-L-Val-Gly-L-Ala-D-Leu-L-Ala-D-Val-L-Val-D-Val-L-Trp-
D-Leu-L-Trp-D-Leu-L-Trp-D-Leu-L-Trp-NHCH$_2$CH$_2$OH.

The transmembrane ionophore is a dimer of Gramicidin-A and
forms a channel through which the ions can diffuse (47-51).
Four models were postulated for the structures of the
dimer. Urry et al (50-53) suggested the N-terminal to N-
terminal structure while the C-terminal to C-terminal model
was preferred by Bradley et al (54). An anti-parallel
double helix structure (55) based on conformational studies
on Gramicidin-A in non-polar organic solvents (56) and a
parallel-β double helix with both N-termini at one end have
also been proposed. Nuclear magnetic resonance studies on
the Gramicidin-A dimer in phosphatidylcholine vesicles (57)
shows a strong N-terminal to N-terminal binding favouring
the first model as the major conformation of this
transmembrane antibiotic. Further studies (58) showed that
the carbonyl groups of the dimer are directed towards the
channel axis and the diameter of the channel is about 4 Å in

the absence of ion occupancy. Thus, the polypeptide and

structural nature of the Gramicidin-A dimer makes it a

suitable model for studying the Sodium channel.

The results presented in this chapter were obtained by

the application of the method described in section 2.4 to

the interaction of ions and molecules with a theoretically

generated structure for the dimer.

3.1 GENERATION OF A STRUCTURE FOR THE GRAMICIDIN-A DIMER

Two methods were used to obtain the atomic coordinates

of the ionophore. The method of Scheraga et al. outlined in

section 2.3.1 was used in both cases to calculate the

configuration of the polypeptide sequence.

The computer program based on this method (59) does not

allow for a $-NH \cdot CH_2 \cdot CH_2 \cdot OH$ end group. Therefore, for

computational purposes, this entity was replaced by

$-NH \cdot CH_3$. The first method, referred to as the 'segmented

approach' is described below.

The fifteen amino acid polypeptide chain was divided

into three consecutive segments of five residues each.

Values for the dihedral angles, except for that about the

peptide bond, for each of the amino acids were taken from

the literature (60-61). The energy of each segment was

calculated as a function of the diheral angles between each

pair of amino acids. For each calculation, these angles

were varied, in turn, by increments of 7.5°. Using this
strategy, the conformation of each segment corresponding to
it's lowest energy was determined.

In order to obtain the geometry of the entire molecule,
the optimised segments were linked sequentially. The
energetically favourable orientation of the linkage between
the pairs of segments was decided by calculating the energy
of the linked segment as a function of the new dihedral
angle formed during the joining of the segments. The
structure of the Gramicidin-A molecule, obtained using the
above strategy, was plotted on a Tektronix T-4015 terminal
adapted with a hard copier. The plot obtained was that of a
globular protein and not a channel, indicating that the
strategy described above was a failure in this particular
application.

In the second method, dihedral angles for the backbone
of polypeptide helices were used to generate a possible
structure for Gramicidin-A. Three helices were chosen (62)
namely (i) the L-D Alanine helix, (ii) the L-D Valine helix
and (iii) a hypothetical helix in which the L-D Ala helical
angles were used for the Gly and Ala residues, the L-D Val
angles for Leu and Val residues and the L-D Phe angles for
the Trp residues. The side chain dihedral angles were not
optimised during the calculation of the conformation of each
of the helices described above. Table 6 gives the energy
corresponding to each conformation.

Table 6 —— CHOICE OF HELIX FOR THE BACKBONE OF GRAMICIDIN-A AND THE CORRESPONDING ENERGY.

CHOICE OF HELIX	ENERGY (kJ/mole)
L-D Ala	8616
L-D Val	23390
L-D Ala + L-D Val + L-D Phe	very large

As the energy calculated for the conformation generated with the first choice of angles was the lowest, this structure for Gramicidin-A was used for all the calculations reported in this thesis.

Figures 1 and 2 are the side and front views of the Gramicidin-A molecules. In the second picture the carbonyl and amino groups of the peptide bond point towards the axis of the channel.

The dimer of Gramicidin-A, which was used as a model for the Sodium channel, is formed from two such monomers. The distance, between the N termini of these moieties which face each other, was varied until a minimum in the energy of interaction between the monomers was obtained. At this point, the second molecule was rotated about the channel
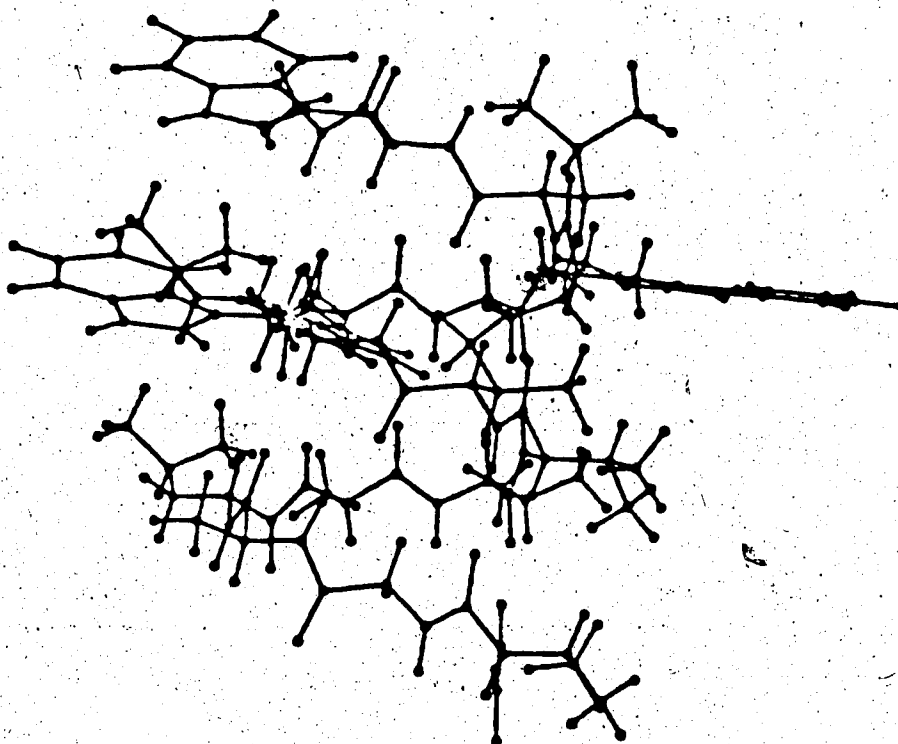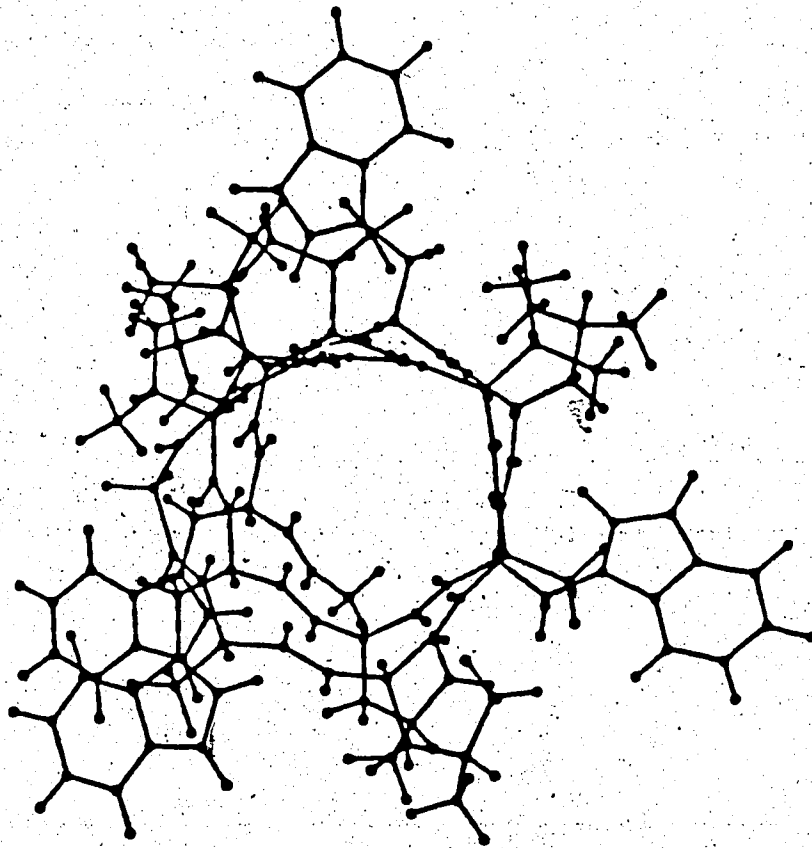
FIGURE 1 - SIDE VIEW OF THE GRAMICIDIN-A MOLECULE.

FIGURE 2 - FRONT VIEW OF THE GRAMICIDIN-A MOLECULE.

axis relative to the first. The angle at which a minimum interaction energy was obtained was taken as that which best described the position of the second molecule in the dimer. The distance between the N-termini of the monomers was calculated to be 2.5 Å, which makes the overall length of the dimer 29.5 Å. This value is in excellent agreement with the experimentally observed value of 30 Å when embedded in a membrane (63) and 32 Å when in methanol or ethanol (64). The angle of rotation of the second monomer relative to the first was 0° and the energy of interaction between the monomers was calculated to be -126.66 kJ/mole.

Figures 3 and 4 show the lateral and front views of the entire ionophore.

3.2 IONIC MOVEMENT THROUGH THE PORE OF THE TRANSMEMBRANE CHANNEL

At present, the Gramicidin-A dimer is the only structurally characterised ion selective transmembrane channel. It is permeable to monovalent cations but does not allow the passage of dications or anions (46). Conductance measurements for the transport of some of the monovalent cations (65) gave the following order for their permeability ratios (given in parenthesis) with respect to Na^+:
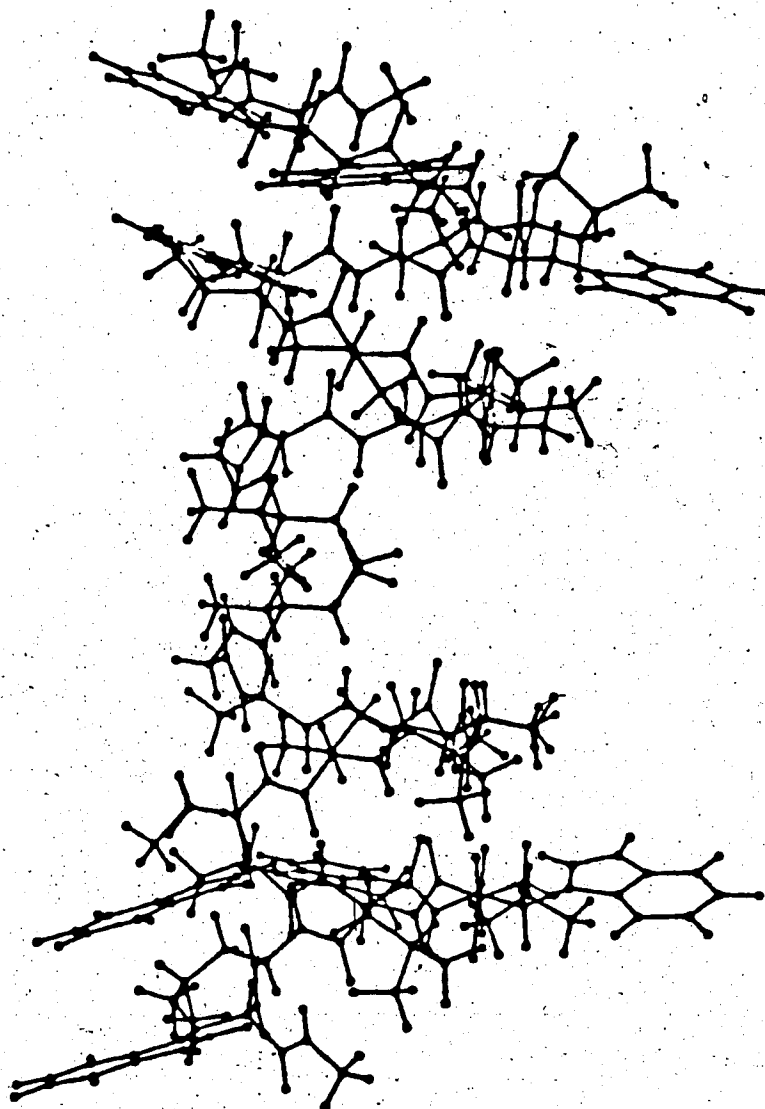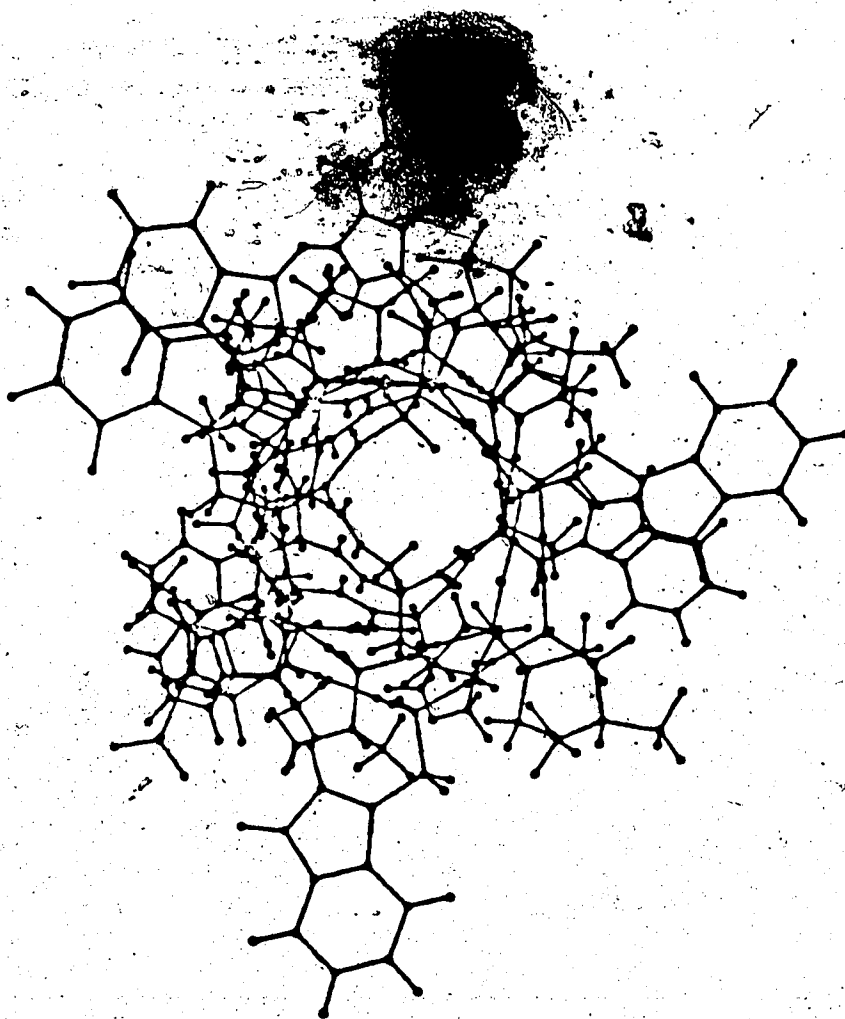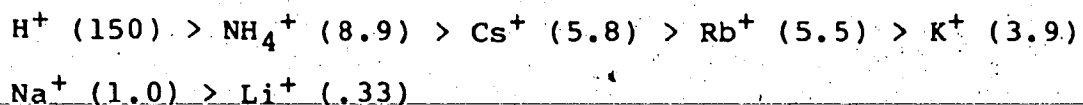
FIGURE 3 - LATERAL VIEW OF THE GRAMICIDIN-A DIMER.

FIGURE 4 - FRONT VIEW OF THE GRAMICIDIN-A DIMER.

H^+ (150) $>$ NH_4^+ (8.9) $>$ Cs^+ (5.8) $>$ Rb^+ (5.5) $>$ K^+ (3.9)

Na^+ (1.0) $>$ Li^+ (.33)

As the diameter of the channel is about 4 Å, a fully hydrated ion will not be able to pass through. Thus, it is a partially hydrated ion that moves through the pore with its vacant hydration sites directly coordinated by the peptide moieties, namely the carbonyl grups, of the ionophore. Effective coordination may require conformation changes in the polypeptide and this mechanism is known as librational motion (66). A consequence of peptide libration is a change in the length and diameter of the channel. As the coordinating group in the peptide is the carbonyl chromophore, the negative charge on the carbonyl oxygen makes the channel selective for cations over anions.

It has been proposed (58) that the proximity of the surrounding lipid is an essential factor in explaining the impermeability of the channel to dications. The single coordination layer provided by the peptide moieties in the backbone of the Gramicidin-A dimer is not sufficient to shield the divalent cation from the lipid around the channel.

The selectivity among the monovalent cations can be explained on the basis of their ionic radii. In Table 7, the ionic radii for the cations studied are listed.

Table 7 IONIC RADII

ION	RADIUS (Å)
Li^+	0.68
Na^+	0.98
K^+	1.33
Ca^{2+}	0.99

The transport of the smaller ions (e.g., Li^+) will require greater coordination by the carbonyl groups and the energetics of the associated changes in the conformation of the polypeptide will make the process less favourable. Hence the low permeability ratio for Li^+.

The free energy profile for the transport of Na^+ through the malonyl gramicidin channel has been determined using Sodium-23 NMR (67-69). Two binding sites, one in each monomer, separated by a distance of 20 Å and a central energy barrier between these sites were observed. Clearly, the value of this central energy barrier will bear a direct relationship to the ease of passage of the ion through the ionophore; the larger the value, the more difficult it will be for the ion to move through the channel. Extending this argument, the energy barrier for the dications should be much larger than that for the alkali ions.

Using the method of calculation described in section

2.4 the movement of an ion X (X = Li^+, Na^+, K^+, Ca^{2+})

through the modified Gramicidin-A dimer was studied. The

new classes, for the interaction of atoms with ions (Table

2), and the corresponding parameters were used for those

atoms comprising the backbone of the polypeptide chain.

For each of the ions studied, the energy profile was

consistent with the experimentally observed two-site binding

theory with a central energy barrier.

In Table 8, the central energy barrier E_c (kJ/mole) and

the distance d (in Å) separating the binding sites are

given. It must be emphasised that in all the calculations

and results described in this chapter, the librational

mechanism of the polypeptide chain has not been included.

Table 8 E_c AND d FOR TRANSPORT THROUGH THE GRAMICIDIN-A

DIMER

ION	E_c (kJ/mole)	d (Å)
Li^+	218	14
Na^+	121	11
K^+	209	12
Ca^{2+}	318	13

Based on the values of E_c, the calculated order of permeability for the ions was:

$$Na^+ > K^+ > Li^+ > Ca^{2+}$$
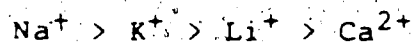
which is not consistent with the experimental observations given above. Besides, this model for the ionophore allows Ca^{2+} to move through the channel when in fact it is found to be a channel poison blocking it, just inside the opening. Figures 5, 6, 7 and 8 show the path taken by Li^+, Na^+, K^+ and Ca^{2+}, respectively.

The environment of the ionophore was modified by simulating the lipid bilayer. Initially, only the polar head group of the lipid molecule was considered. Formic acid was chosen for this purpose and its geometry obtained from X-ray data (70).

Twelve molecules of formic acid were placed, one at a time, around the mouth of a Gramicidin-A molecule. The position of the n-th formic acid molecule is that one corresponding to the lowest interaction energy with the Gramicidin-A and the (n-1) formic acid molecules already present. Figure 9 is a plot of Gramicidin-A with the surrounding molecules of formic acid and in figure 10 only the formic acid molecules are shown for clarity. The dimer of the modified channel was obtained in the same manner as for the Gramicidin-A dimer. The energy of interaction
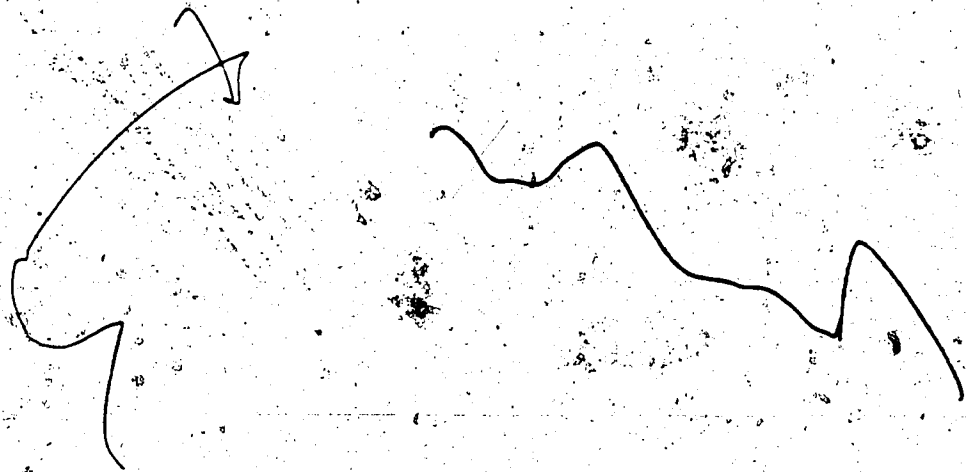
FIGURE 5 - FRONT AND LATERAL VIEW OF PATH TAKEN BY Li$^+$.

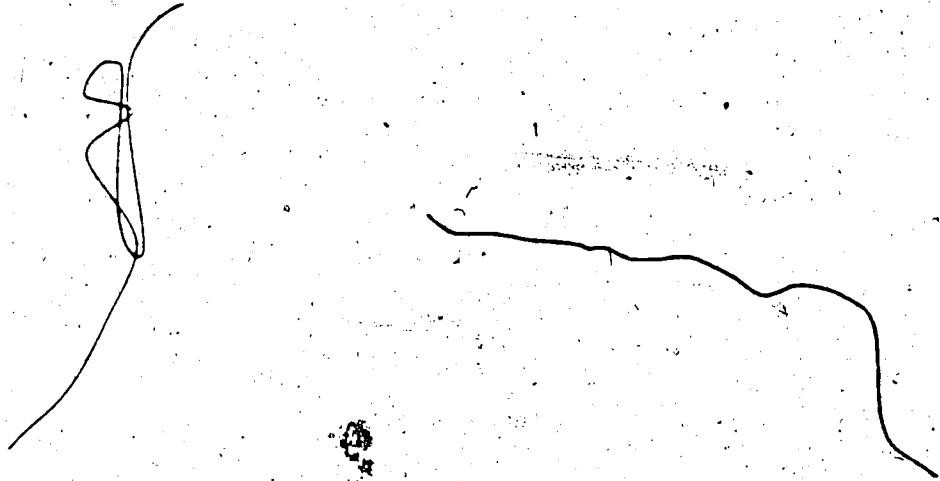FIGURE 6 - FRONT AND LATERAL VIEW OF PATH TAKEN BY Na$^+$.

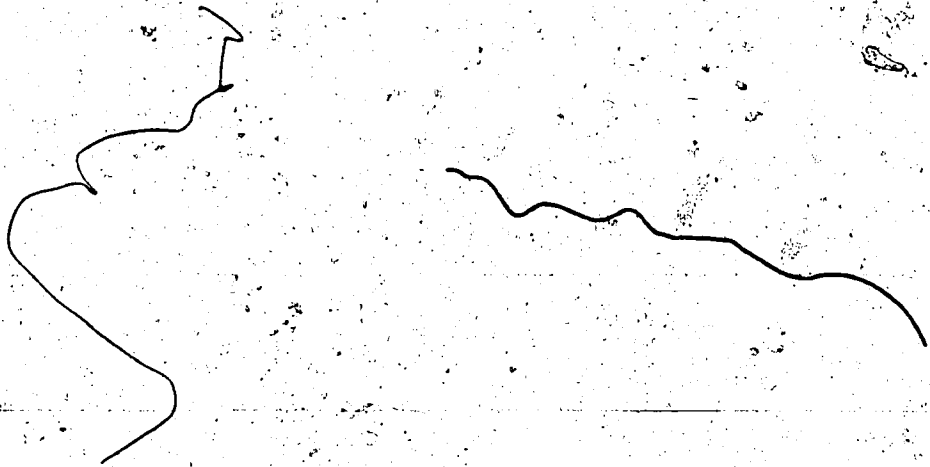FIGURE 7 - FRONT AND LATERAL VIEW OF PATH TAKEN BY K^+.

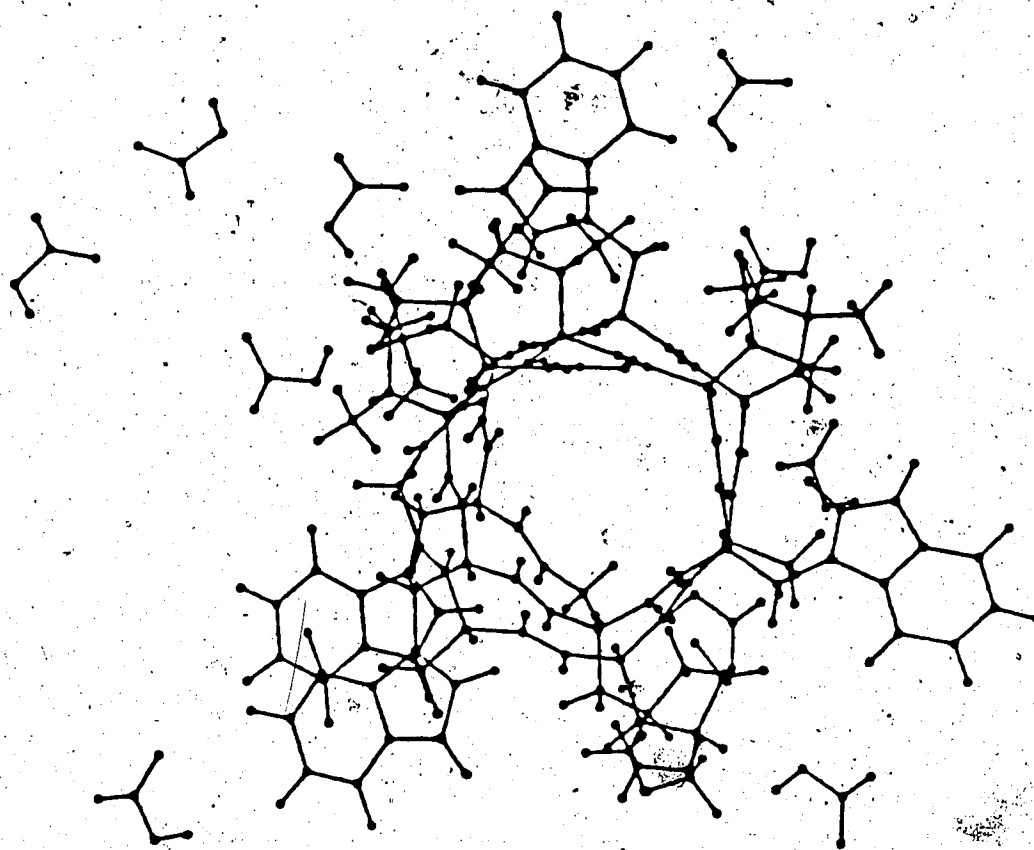FIGURE 8 - FRONT AND LATERAL VIEW OF PATH TAKEN BY Ca^{2+}.

FIGURE 9 — FRONT VIEW OF GRAMICIDIN-A WITH FORMIC ACID
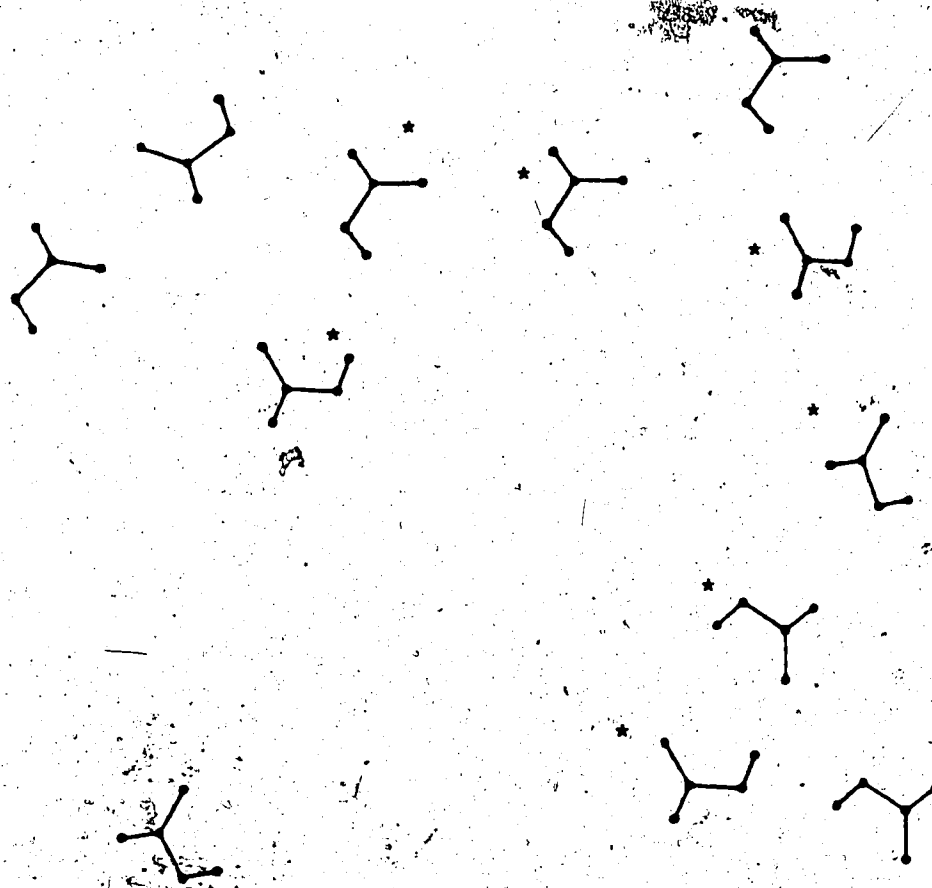MOLECULES.

FIGURE 10 - CLUSTER OF FORMIC ACID MOLECULES AROUND THE PORE.

between the monomers was -127.16 kJ/mole. The lateral and

front views of the entire modified dimer are shown in

figures 11 and 12, respectively.

In order to study the transport of ions through the

modified channel, it was necessary to reassign the atoms in

the acid molecules closer to the mouth of the channel to the

new classes. This was done in order to take the ionic

nature of the interactions into accout. The molecules whose

atoms were reassigned are indicated by an asterix in figure

10.

Each of the ions, Li^+, Na^+, K^+ and Ca^{2+} were placed

just inside the pore of the modified channel and allowed to

find their paths of minimum energy. In each case the ions

were pushed out of the channel. This showed the existence

of a positive energy gradient which the ions could not

overcome and the inadequacy of the formic acid molecules in

describing the lipid bilayer.

A further refinement was carried out by placing four

molecules of octane per modified monomer, under the network

of acid molecules so as to simulate a lipid environment

around the polypeptide chain. The result for a monomer is

shown in figure 13. Figure 14 shows the pore of the monomer
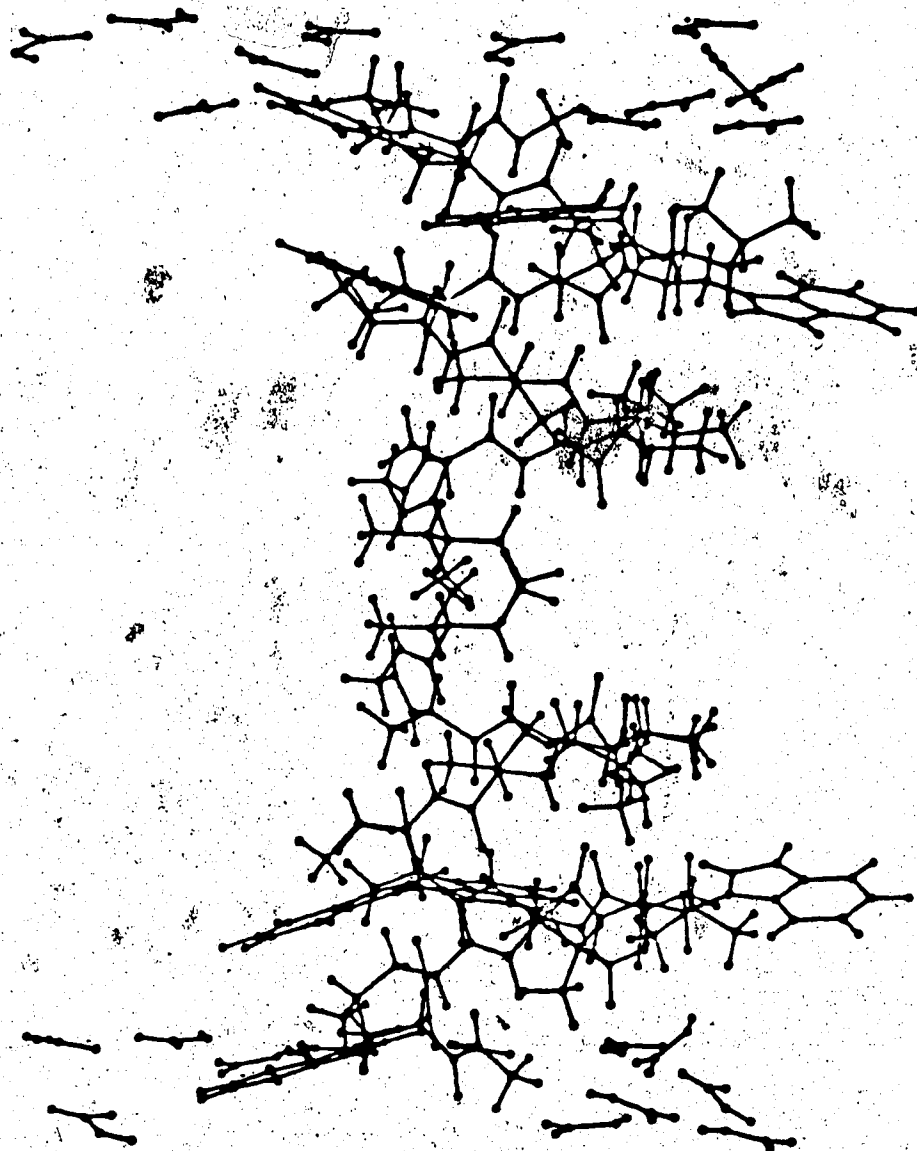
in the refined model.

FIGURE 11 - LATERAL VIEW OF THE GRAMICIDIN-A DIMER WITH
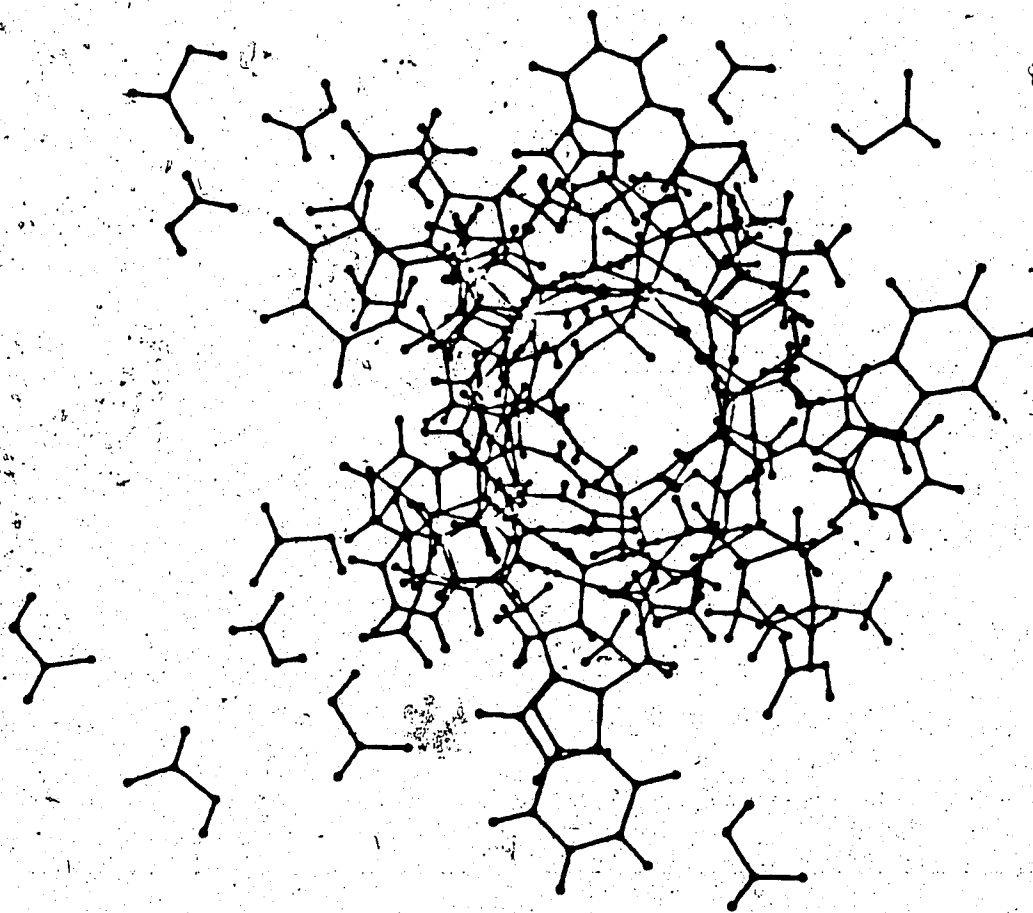THE SURROUNDING MOLECULES OF FORMIC ACID.

FIGURE 12 - FRONT VIEW OF THE GRAMICIDIN-A DIMER WITH THE
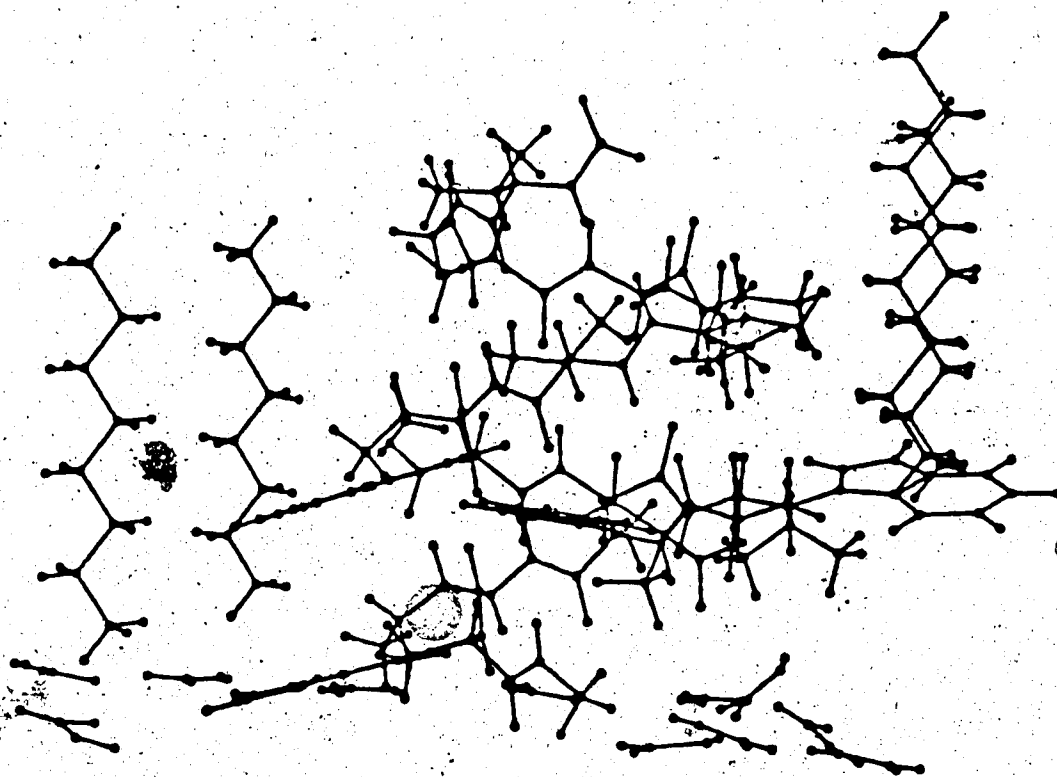SURROUNDING MOLECULES OF FORMIC ACID.

FIGURE 13 - SIDE VIEW OF THE REFINED MODEL OF A
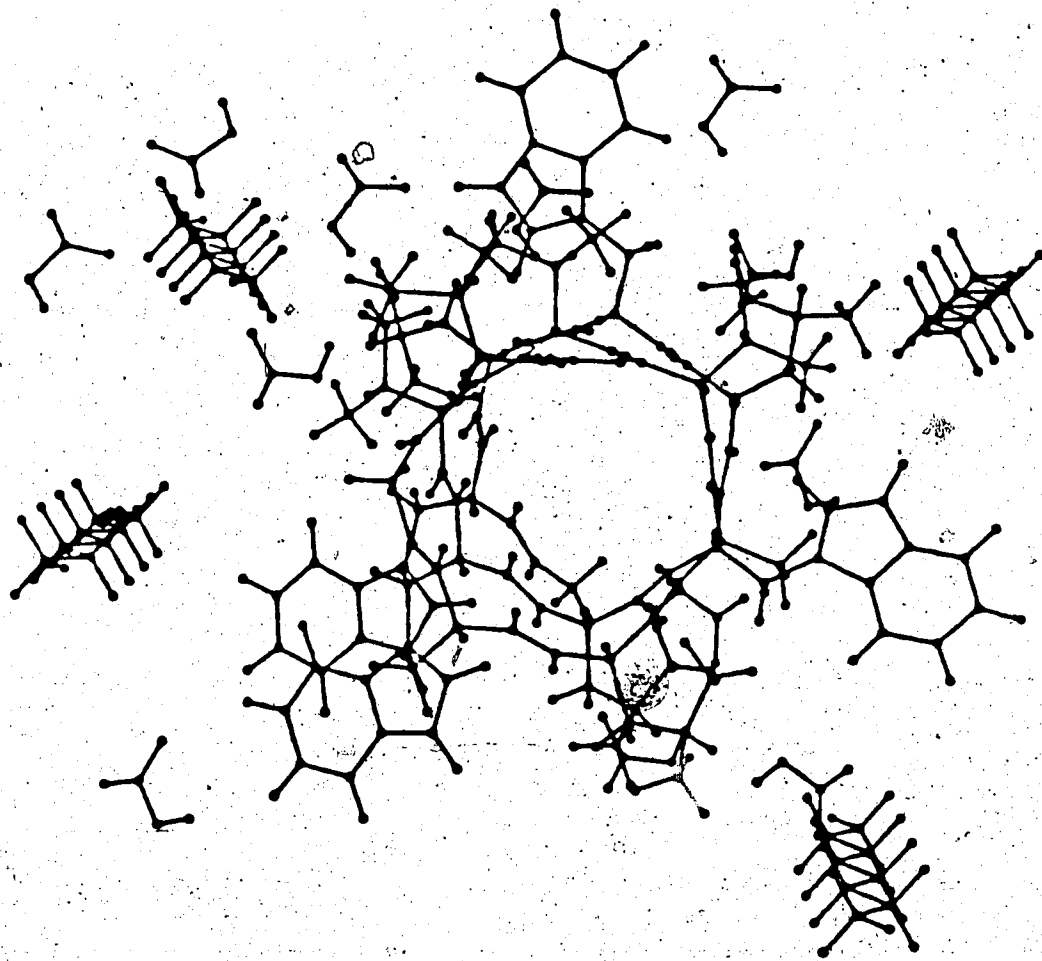GRAMICIDIN-A MONOMER.

FIGURE 14 - THE PORE OF THE REFINED MODEL FOR GRAMICIDIN-A.

As proposed by Urry et al. (71), a compressing of the lipid layer at the site of the transmembrane channel was included by moving the entire simulated lipid environment (i.e., formic acid and octane molecules) by a distance of 1.5 Å. This value of 1.5 Å was chosen arbitrarily.

The dimer of two such molecules was then considered to represent the transmembrane channel, embedded in a lipid bilayer. The interaction energy between the halves was evaluated using the same strategy for dimerisation as in the previous cases. The value of the interaction energy obtained was -145.67 kJ/mole. Figures 15 and 16 show the side and front views of the channel.

The ions under consideration were allowed to move in the ionophore under the potential created by the dimer. Table 9 gives the central energy barriers (E_c) and the distances (d) between the two binding sites.

Table 9 E_c AND d FOR TRANSPORT THROUGH THE REFINED MODEL

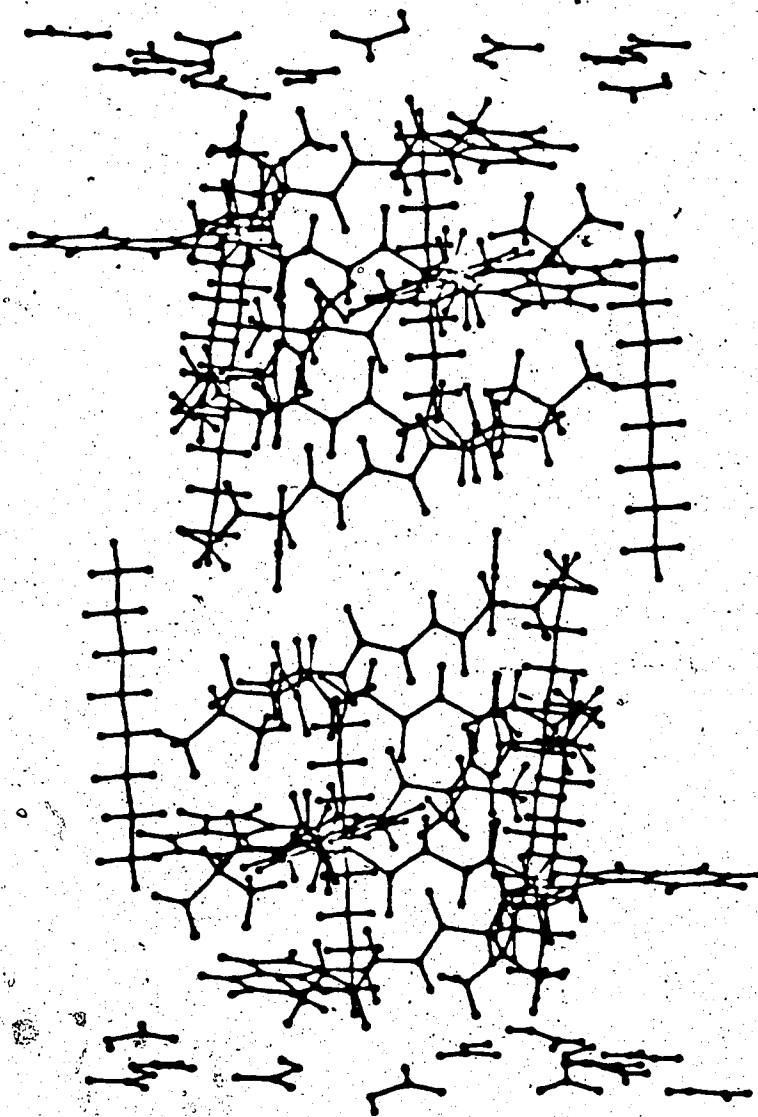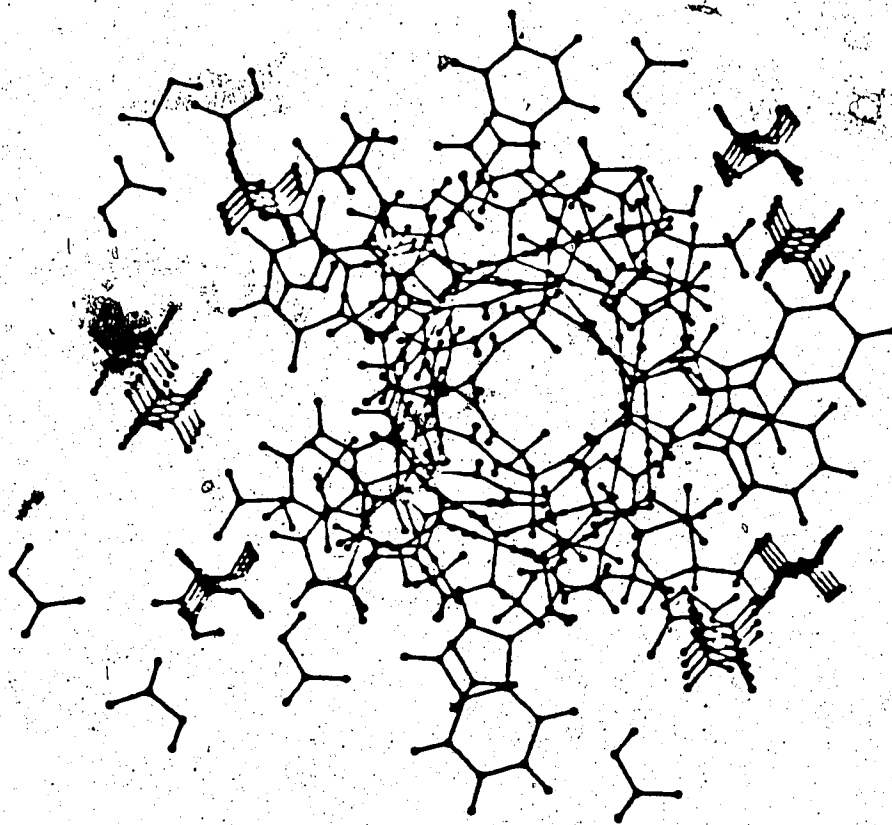| ION	E_c (kJ/mole)	d (Å)
Li^+	265	12
Na^+	140	11
K^+	132	12
Ca^{2+}	very large	

FIGURE 15 - SIDE VIEW OF THE REFINED CHANNEL.

FIGURE 16 - FRONT VIEW OF THE REFINED CHANNEL.

The predicted order of permeability is $K^+ > Na^+ > Li^+$
$>>> Ca^{2+}$ in excellent agreement with experiment. The
channel poisoning nature of Ca^{2+} is amply illustrated by the
very high energy of interaction $(.29 \times 10^6$ kJ/mole) at a
distance of about 1.5 Å from the pore, inside the channel.
Figures 17, 18 and 19 show the path of Li^+, Na^+ and K^+
through the pore of the refined model for the transmembrane
channel.

The final refinement to the model consisted of
including a chain of water molecules in the pore, as
observed by Finkelstein (72). Six molecules of water, three
in each monomer, were arranged one at a time in the pore of
the channel. The first water molecule was placed just
outside the mouth of the channel at the position which gave
the lowest energy of interaction. The same criterion was
used in arranging the others, the sixth molecule being just
outside the other end of the channel.

As in the previous cases, the movement of the ions
through the solvated pore was determined and the central
energy barriers (E_c) and distance of separation (d) of the
binding sites evaluated. The corresponding values are
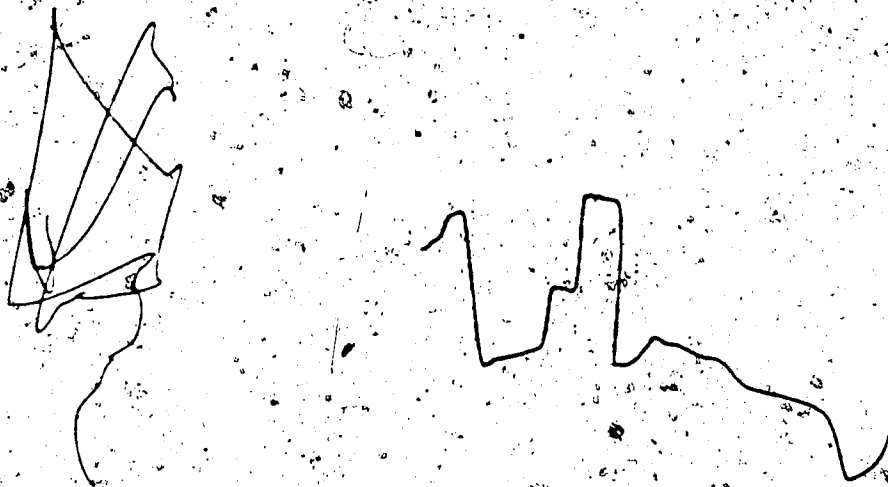listed in Table 10.

FIGURE 17 – FRONT AND LATERAL VIEW OF THE PATH OF Li$^+$

THROUGH THE PORE OF THE REFINED MODEL.

FIGURE 18 – FRONT AND LATERAL VIEW OF THE PATH OF Na$^+$

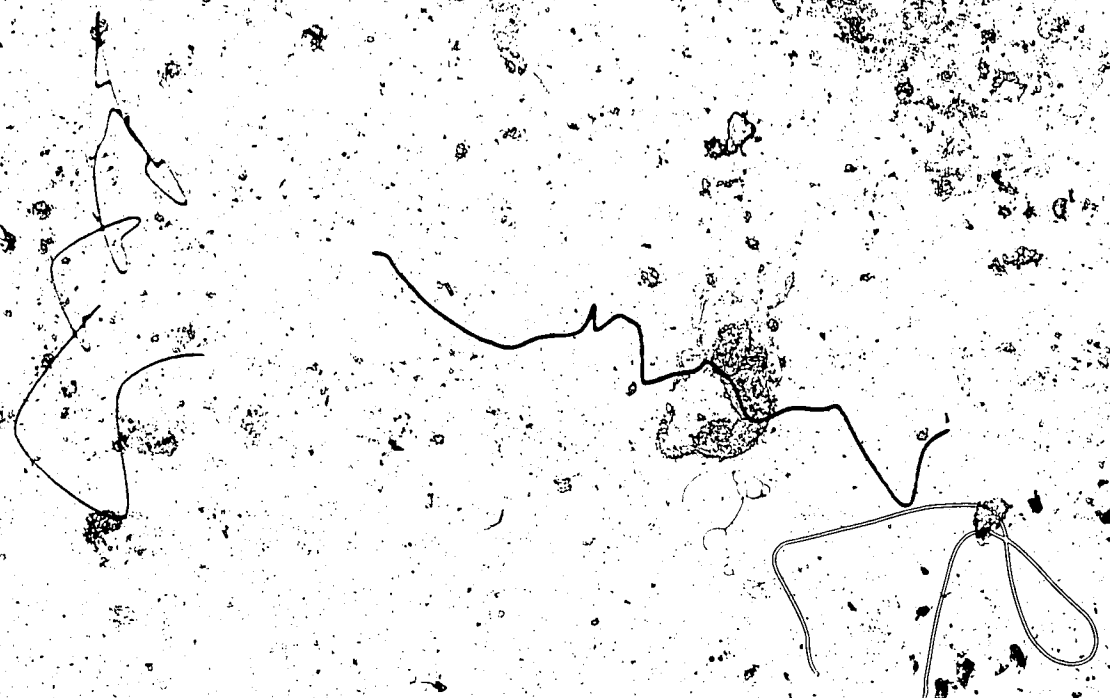THROUGH THE PORE OF THE REFINED MODEL.

FIGURE 19 - FRONT AND LATERAL VIEW OF THE PATH OF K^+

THROUGH THE PORE OF THE REFINED MODEL

TABLE 10 E_C AND d FOR TRANSPORT THROUGH THE SOLVATED PORE.

ION	E_C (kJ/mole)	d (Å)
Li^+	222	3
Na^+	121	
K^+		
Ca^{2+}	very large	

The channel poisoning nature of Ca^{2+} is shown again in this model. The improvement to the model by including water molecules in the pore is demonstrated by the fact that the passage of K^+ is hindered. In other words, with the fixed conformation for the polypeptide chain and simulated lipid and hydration environment, the potassium ion does not pass through the pore. This observation is an indication of the importance of peptide libration in ionic transport. Koeppe et al. (73) have reported that the binding of K^+ to the channel widens the channel diameter to 6.8 Å while shortening its length from 32 Å to 26 Å.

The results presented in this section illustrate the improvements to the model of the transmembrane channel according to their manifestations on the transport parameters E_C and d. With each stage of improvement, the

agreement between the calculated and experimental

permeability trends was better. However, the distance

separating the binding sites was not comparable with the

experimental value of 20 $\mathring{A}$ obtained for Na^+ (67-69).

The spiral nature of the movement of the ions when

viewed along the channel axis (Figures 5-8, 17-19), indicate

that the ions coordinate with the carbonyl groups during

transport. This observation shows that peptide libration

should be considered in any further improvements to the

simulation of ionic transport.

3.3. INTERACTION OF THE CHANNEL WITH MOLECULES.

In the preceeding section, a model for the

transmembrane channel embedded in a lipid was refined in

stages and the transport properties of certain ions through

the pore of this channel studied. As discussed in section

3.2, the last refinement, which included a chain of water

molecules through the pore, best described the energy

profiles for the movement of these ions. It is this final

model which is used to study interactions between the

channel and certain molecules of biological interest.

The importance of ionic transport in initiating the

action potentials has been discussed in the first chapter of

this thesis. Interference with the transport of an ion

affects its concentration ratio within and outside the

cell. This has a direct influence on the action potential which in turn effects the release of neurotransmitters into the synaptic cleft. Thus, a molecule which hinders the passage of ions through the pore by blocking the channel will inhibit nervous transmission. That is, a neurotoxin can be thought of as a molecule, which, being strongly attached to the mouth of the channel effectively blocks the pore restricting the migration of ions through the transmembrane channel.

On the other hand, a molecule which interacts weakly with the channel would have a temporary inhibitory effect on the release of neurotransmitters. Thus, the interaction between molecules which induce general anesthesia and the channel pore can be considered to be weak. In addition, the blocking of the channel pore by such molecules needs not interrupt completely the ionic transport.

3.3.1 TOXICITY OF TETRODOTOXIN AND SAXITOXIN

The marine toxins, tetrodotoxin and saxitoxin (Figure 20), have been known to block the conduction of nerve impulses along an axon.
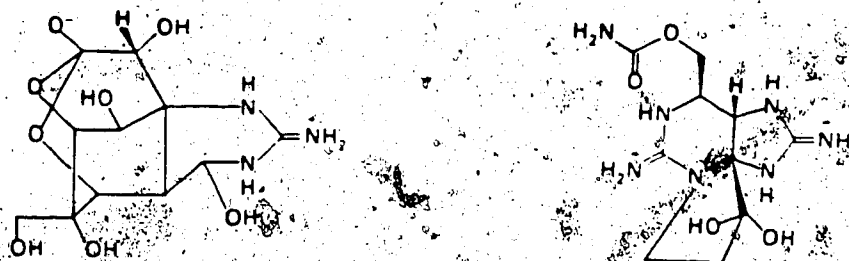
FIGURE 20. STRUCTURES OF TETRODOTOXIN (LEFT) AND SAXITOXIN (RIGHT).

Their toxic nature has been related to the very strong binding to the Sodium channel and the common structural entity, the guanidinium ion, associated with this channel blocking character (42,74). This hypothesis assumes that the guanidinium ion behaves like Na^+ in its interactions with the pore but its penetration of the channel inhibited by the bulky structure of the rest of the toxin.

Before studying the interactions of the toxins with the model for the Sodium channel, it was decided to investigate the interactions of the guanidinium entity with the channel pore. An optimised structure for the guanidinium ion obtained from a self-consistent field calculation using a 6-31G basis set (75) was used to calculate the interaction energy between the solvated channel and the guanidinium

fragment. The lowest interaction energy obtained was
-550.88 kJ/mole and the position of the ion was found to be
inside the layer of formic acid molecules and just outside
the mouth of the Gramicidin-A pore as shown in figure 21.
When viewed along the channel axis, the guanidinium ion was
found to block the pore (figure 22). The large interaction
energy in this case illustrates the possible implications of
such int   in the toxicity of the marine toxins as
discuss

The tetrodotoxin and saxitoxin molecules were treated
in a similar manner. The geometry of the former molecule
was obtained from X-ray data (76) and the coordinates of
saxitoxin calculated from standard geometries. The
interaction energy for tetrodotoxin and saxitoxin with the
pore of the refined Gramicidin-A dimer model was evaluated
to be -441.14 kJ/mole and -323.57 kJ/mole. Figures 23, 24
and 25, 26 give the lateral and front views for the
interactions of tetrodotoxin and saxitoxin with the mouth of
the pore, respectively.

From figures 24 and 26, it is clear that in both toxins
it is the guanidinium entity that preferentially interacts
with the channel, blocking the transport of ions. This
observation is in good agreement with the hypothesis
proposed by Hille (74). Also the interaction energies for
each toxin with the channel is comparable with the
energetics of bond formation as listed in Table 11.
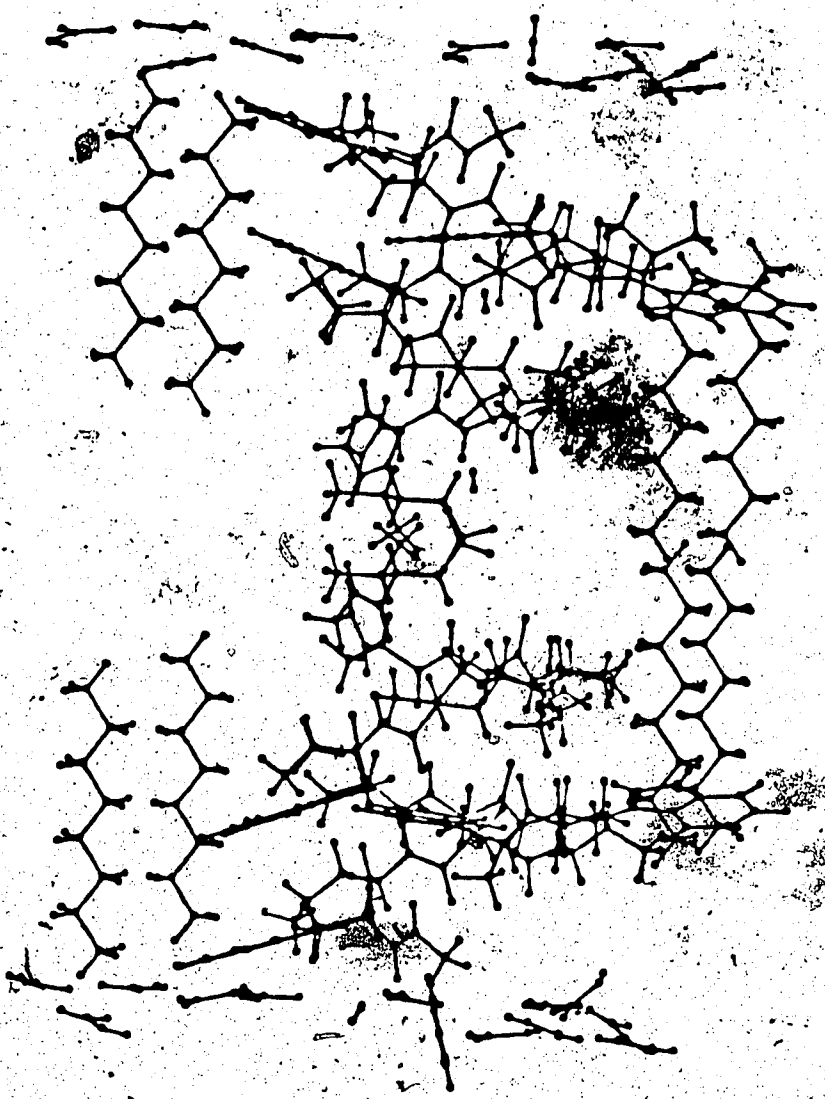
FIGURE 21 - POSITION OF THE GUANIDINIUM ION AT THE MOUTH
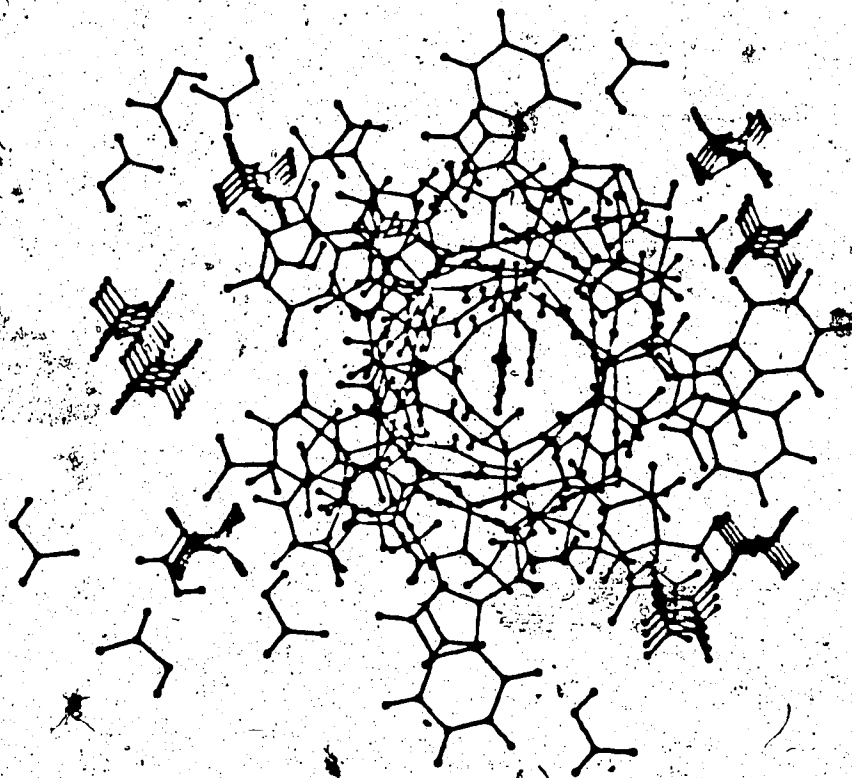OF THE CHANNEL.

FIGURE 22 - CHANNEL BLOCKING CHARACTERISTIC OF THE
GUANIDINIUM ION.

FIGURE 23 - LATERAL VIEW OF THE INTERACTION OF
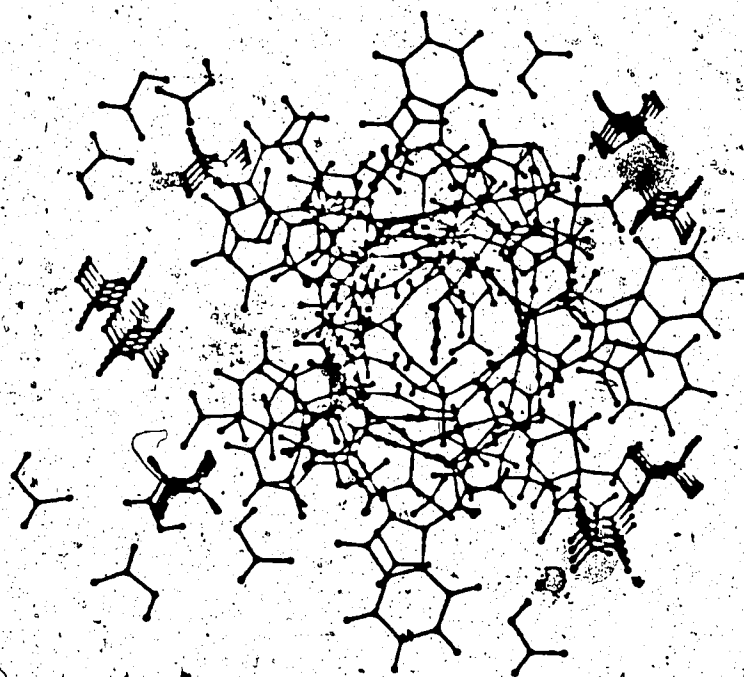TETRODOTOXIN WITH THE CHANNEL.

FIGURE 24 - FRONT VIEW OF THE INTERACTION OF
TETRODOTOXIN WITH THE CHANNEL.
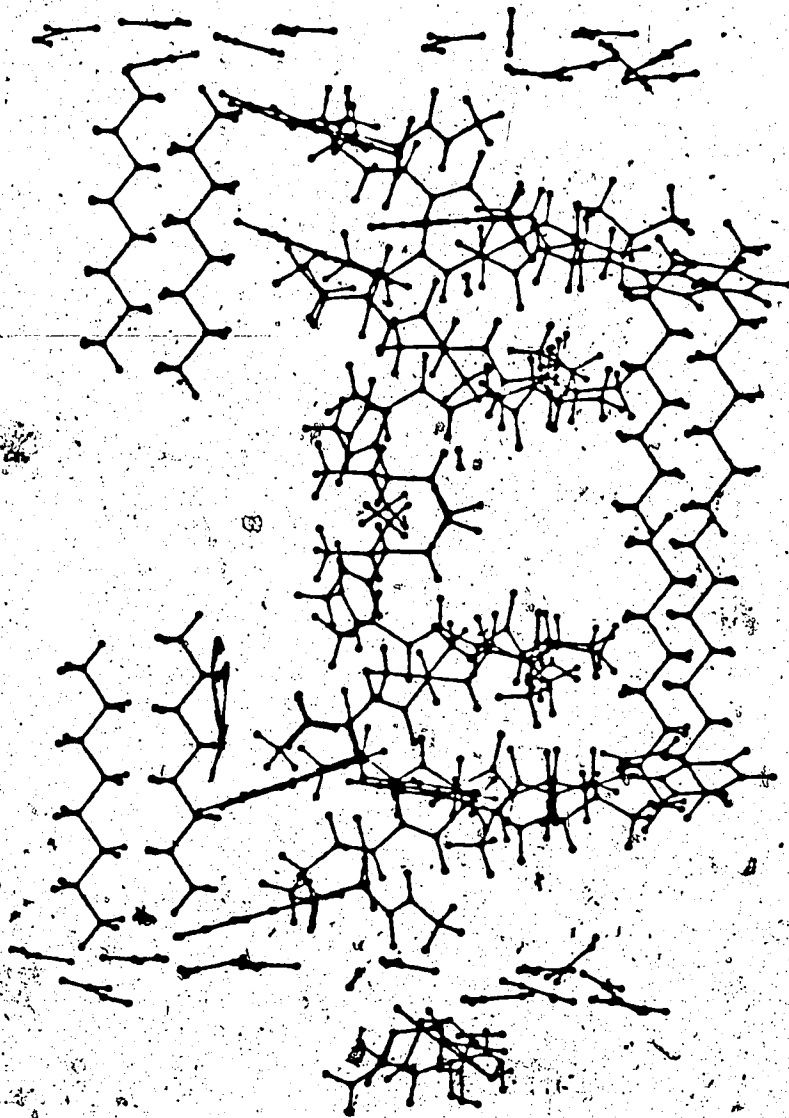
FIGURE 25 - SIDE VIEW OF THE INTERACTION OF SAXITOXIN
WITH THE CHANNEL.
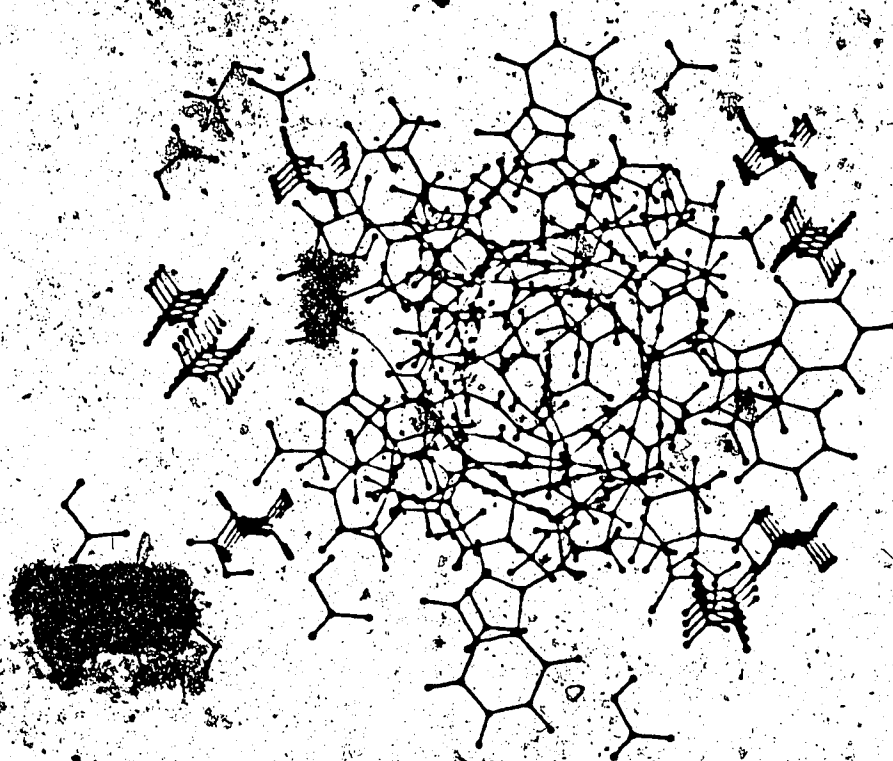
FIGURE 26 - FRONT VIEW OF THE INTERACTION OF SAXITOXIN
WITH THE CHANNEL.

TABLE 11   ENERGIES FOR CERTAIN BONDS

BOND	BOND ENERGY (77) (kJ)
F-F	156.9
N-H	314.0
Me-H	435.0

Comparing the values obtained for the interaction energy of the toxins with the bond energies listed above, the interaction of these toxins with the pore of the model for the Sodium channel can certainly be classified as strong, thus illustrating the toxic nature of the two marine toxins.

3.3.2   INTERACTION OF ANESTHETIC MOLECULES

It has been postulated (9) that molecules which interfere reversibly with the conductance properties of the Sodium channel induce anesthesia. The interference could be due to a partial or complete blocking of the Sodium channel. Moreover, the interaction energy accompanying such a channel block would be expected to be in the thermal range and can be compensated by molecular collisions and conformational changes in the systems concerned.

Diethyl ether is a common anesthetic and the above hypothesis for a mechanism of anesthesia was studied by evaluating the interaction energy between the ether and the channel pore. The coordinates of the ether were obtained from X-ray crystallographic studies (78). The interaction energy of interest was obtained as in the previous cases - i.e., by specifying various positions for the ether molecule relative to the channel. The lowest energy of interaction calculated was -78.00 kJ/mole and the position of the ether molecule is as shown in figure 27. The view along the channel axis (figure 28) shows the partial blocking of the channel by diethyl ether.

The biochemical environment of the Sodium channel would have many molecules of water in the vicinity of the mouth of the pore. The incoming ether molecule has to compete with these water molecules in order to effectively block the channel. If the interaction of a molecule of ether with the mouth of the channel is more favourable than the corresponding interaction of a molecule of water, when placed at the same position as the ether, the water will be displaced by the ether.

The interaction energy for a water molecule with the pore, at the same position that gives the best energy of interaction for the ether, was evaluated to be -69.53 kJ/mole. This result shows that a molecule of ether has a preferred interaction with the channel than a water molecule
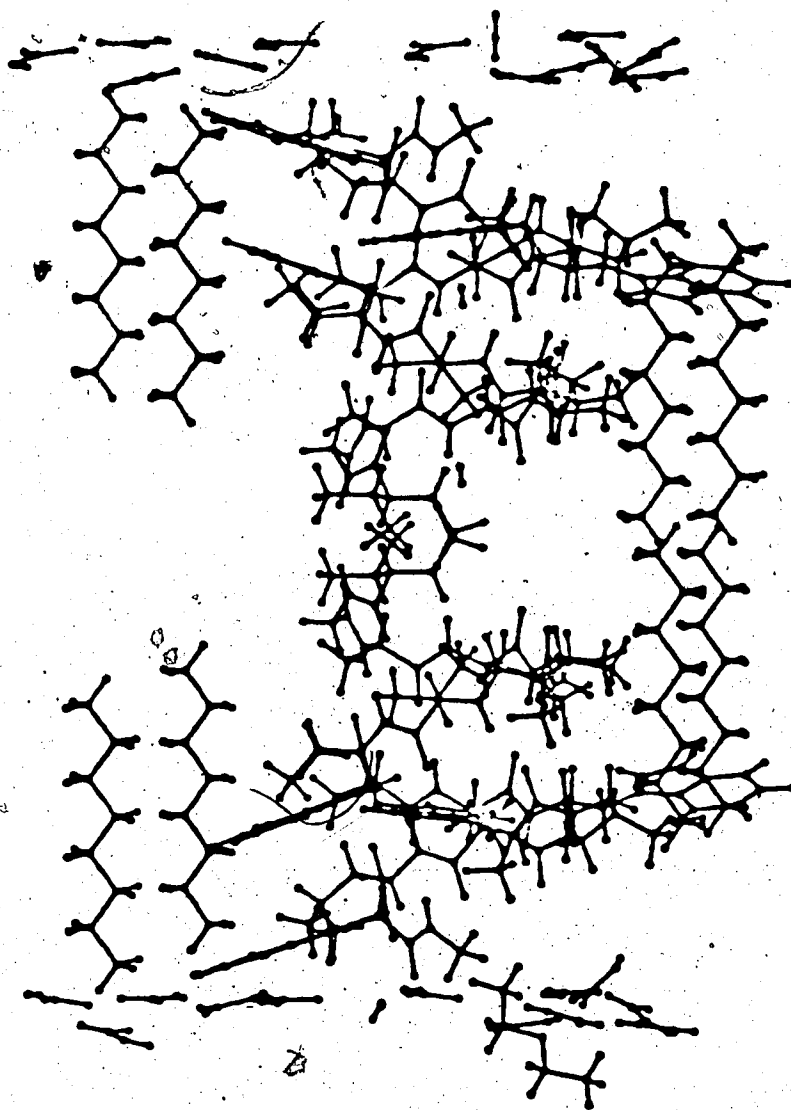
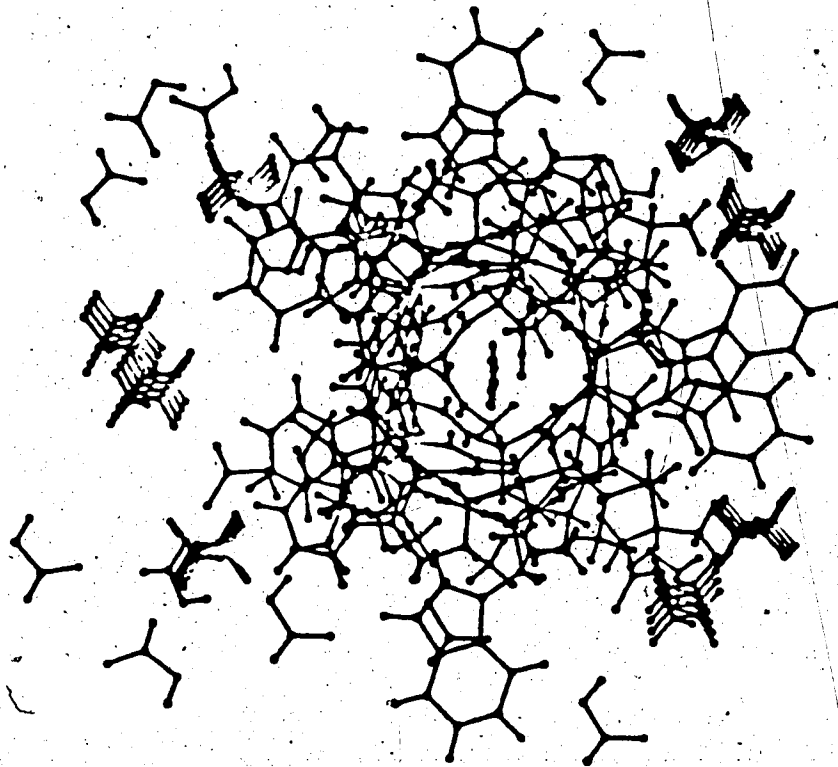FIGURE 27 - INTERACTION OF DIETHYL ETHER WITH THE

CHANNEL PORE.

FIGURE 28 — PARTIAL BLOCKING OF THE PORE BY THE ETHER.

at that position. In other words, diethyl ether can
displace water for effective interaction with the mouth of
the pore. Besides, the values for the interaction energies
are in the thermal range which indicates that such
interactions are reversible - a requisite for a postulated
mechanism of anesthesia.

Another approach in outlining a mechanism of general
anesthesia is to consider the possible interactions in the
synaptic cleft. Extracellular Na^+, water and, during nerve
impulse, a high concentration of neurotransmitter would be
some of the species found in the synaptic cleft.
Interference with the conduction of the nerve impulse
implies that the neurotransmitter is not available in its
free form to depolarise the post-synaptic membrane. If the
molecules of ether have a preferred interaction with the
neurotransmitter than with water or the extracellular Sodium
ions, it can be postulated that such interactions in the
synaptic cleft may be responsible, in addition to the
channel blocking property, for the inducement of anesthesia.

This hypothesis was tested by evaluating the energies
of interaction of a Sodium ion, water and acetylcholine with
a cluster of ether molecules. In each case, an ether
molecule was allowed to interact with the other system
(i.e., Na^+, water or acetylcholine) until the best value for
the energy minimum was obtained in the steepest descent
procedure. Additional ether molecules were clustered around

the initial supersystem and the energy of interaction for each new molecule evaluated.

Table 12 gives these values (in kJ/mole) for the interaction of five molecules of diethyl ether, one at a time, with Na^+, acetylcholine and water.

TABLE 12   INTERACTION ENERGIES (kJ/mole) OF Na^+, ACETYLCHOLINE AND WATER WITH DIETHYL ETHER.

SPECIES	Na^+	ACETYLCHOLINE	WATER
ETHER			
1	-151	-379	-33
2	-1025	-1064	-1
3	-337	-1437	
4	-455	-848	
5	-531	-281	

Although the results listed in Table 12 are preliminary by nature, there is a clear indication of the preferred interaction between the cluster of ether molecules and acetylcholine over the corresponding interactions with Na^+ or water. This trend shows that the possible interactions in the synaptic cleft should be considered along with the channel blocking property of anesthetics in formulating a mechanism of general anesthesia.

CHAPTER 4 - CONCLUSIONS

The results of the calculations presented in this thesis illustrate the applicability of a 1/R expansion in studying interactions between systems participating in biochemical processes. As the results have been discussed in the relevant sections of Chapter 3, only general comments on the applicability of the method and improvements to the theory will be presented here.

The agreement between the calculated and experimental ordering of the permeabilities of the ions improved with each refinement of the simulation of the Sodium channel. The model with the solvated pore best described the passage of the ions through the channel. Nevertheless, for the transport of Na^+, the distance between the two binding sites was not in agreement with the experimental observation of 20 A. This may be due to many factors, among them the inadequate representation of the biological nature and environment of the channel and the neglect of the peptide libration. The introduction of peptide libration may change this parameter of ionic transport as the movement of the channel backbone to effectively coordinate the ion results in conformational changes of the Gramicidin-A dimer.

In all the results on ionic movement presented in the previous chapter, the charge on the ion is assumed to be unity for the alkali ions and two for the Calcium ion. During ionic transport, this charge may be delocalised over the amino acid residues and other molecular species, like water, present in the vicinity of the ion. Calculations (79) using the complete neglect of differential overlap (CNDO) method indicated that such charge transfers are possible and result in the stabilisation of the systems concerned.

A further refinement to the channel model would consist of replacing the simulated polar headgroups by phosphate moieties. Such a treatment requires the evaluation of the f and g parameters for phosphorous and the associated oxygen atoms. The ab-initio study (80) of the interaction of the phosphate group with water can be used to evaluate the required parameters. Simulation of the lipid environment of the ionophore by phospholipid molecules is a further improvement to the model but the computational requirements would be extremely large.

The results obtained for the interaction of the toxins with the channel illustrate the strong binding between the toxin and the mouth of the pore in agreement with recent experimental studies (81). The studies on diethyl ether illustrate some of the interactions which may be responsible for the inhibition of nervous transmission. Similar studies

on related anesthetics like methoxyflurane and isoflurane could substantiate the importance of the postulated interactions in inducing anesthesia. However, such studies require the evaluation of the f and g parameters for the Fluorine and Chlorine atoms of methoxyflurane and isoflurane. In order to determine the parameters, good ab-initio calculations for the interactions of these atoms with systems whose atoms can be assigned to known classes are required. This is the major drawback in the applicability of the method presented in this thesis.

The correlation energy defined within a variational treatment of interacting systems can be associated with the dispersion energy that can be derived in a perturbation analysis of weak interactions (82). As mentioned in section 2.2.3.2, this dispersion energy can be expressed as a function of the $(R^{-6} + R^{-8} + R^{-10})$ terms if the dipole-quadrupole and quadrupole-quadrupole contributions are considered, in addition to the dipole-dipole interaction term. Therefore, inclusion of the $(R^{-8} + R^{-10})$ terms takes into account a major portion of the intersystem correlation energy. The coefficients of these two terms would require suitable parameterisation in a manner analogous to that used for the R^{-1}, R^{-4}, R^{-6} and R^{-12} terms. The study by Lie et al (83) makes use of such a formulation together with the Hartree-Fock potential to simulate the structure of bulk water.

The applicability of the method of calculation is
demonstrated by the results presented in the previous
chapter of this thesis. The computational requirements are
modest, even for the study of such large systems like the
Gramicidin-A dimer. Within the framework of the theory, the
results obtained using the potential energy function are
useful in understanding interactions between biomolecules.

REFERENCES

1. A.L. Stanford Jr. "Foundations of Biophysics", Academic Press, (1975).

2. C.F. Stevens, Sci. Am. **241**, 49 (1979).

3. L. Stryer, "Biochemistry", W.H. Freeman & Co., (1981).

4. A.L. Hodgkin and A.F. Huxley, Nature (London) **144**, 710 (1939).

5. A.L. Hodgkin and A.F. Huxley, Cold Spring Harbor Symp. Quant. Biol. **17**, 43 (1952).

6. A.L. Hodgkin and A.F. Huxley, J. Physiol. (London) **116**, 449 (1952).

7. A.L. Hodgkin, A.F. Huxley and B. Katz, Arch. Sci. Physiol. **3**, 129 (1949).

8. C.W. Myers and D.W. Daly, Sci. Am. **248**, 120 (1983).

9. "Molecular Mechanisms of Anesthesia", Progress in Anesthesiology, Vol. 2, Ed. B.R. Fink, Raven Press (1980).

10. M. Born and J.R. Oppenheimer, Ann. Physik, **84**, 457 (1927).

11. C.C.J. Roothan, Rev. Mod. Phys. **23**, 69 (1951).

12. F. London, Z. Phys. **63**, 245 (1930).

13. F. London, Z. Phys. Chem. B. **11**, 221 (1930).

14. F. London, Trans. Farad. Soc. **33**, 8 (1937).

15. J.O. Hirschfelder, C.F. Curtiss and R.B. Bird, "Molecular Theory of Gases and Liquids", John Wiley, New York, (1964).

16. J.E. Lennard-Jones, Proc. Roy. Soc. A106, 441, 463 (1924).

17. J.C. Slater and J.G. Kirkwood, Phys. Rev. 37, 682 (1931).

18. D.R. Bates "Quantum Theory", Vol. 1, Academic Press, New York, p.280 (1961).

19. C. Mavroyannis and M.J. Stephen, Mol. Phys. 5, 629 (1962)

20. F.A. Momany, G. Vanderkooi and H.A. Scheraga, Proc. Natl. Acad. Sc. 61, 429 (1968).

21. F.A. Momany, R.F. McGuire and H.A. Scheraga, J. Phys. Chem. 76, 375 (1972).

22. F.A. Momany, R.F. McGuire, A.W. Burgess and H.A. Scheraga, J. Phys. Chem. 79, 2361 (1975).

23. F.A. Momany, L.M. Carruthers and H.A. Scheraga, J. Phys. Chem. 78, 1621 (1974).

24. F.A. Momany, L.M. Carruthers, R.F. McGuire and H.A. Scheraga, J. Phys. Chem. 78, 1595 (1974).

25. J.A. Pople, D.A. Santry and G.A. Segal, J. Chem. Phys., 43, S129 (1965).

26. W.P. Minicozzi and D.F. Bradley, J. Compt. Phys. 4, 118 (1969).

27. T. Ooi, R.A. Scott, G. Vanderkooi and H.A. Scheraga, J. Chem. Phys. **46**, 4410 (1967).

28. E. Clementi, F. Cavallone and R. Scordamaglia, J. Am. Chem. Soc. **99**, 5531 (1977).

29. R. Scordamaglia, F. Cavallone and E. Clementi, J. Am. Chem. Soc. **99**, 5545 (1977).

30. G. Bolis and E. Clementi, J. Am. Chem. Soc. **99**, 5550 (1977).

31. E. Clementi, Int. J. Quant. Chem. **3S**, 179 (1970).

32. Technical Report TC-AR-I-81, Division of Theoretical Chemistry, Department of Chemistry, The University of Alberta (1981).

33. S. Fraga, J. Comp. Chem. **3**, 329 (1982).

34. G. Corongiu, E. Clementi, E. Pretsch and W. Simon, J. Chem. Phys. **70**, 1266 (1979).

35. H. Popkie and E. Clementi, J. Chem. Phys. **57**, 1077 (1972).

36. H. Kistenmacher, H. Popkie and E. Clementi, J. Chem. Phys. **58**, 1689 (1973).

37. H. Tatewaki and S. Huzinaga, J. Comp. Chem. **1**, 205 (1980).

38. S. Fraga, K.M.S. Saxena and J. Karwowski, "Hartree-Fock Atomic Data" (1975).

39. S.F. Boys and F. Bernadi, Mol. Phys. **19**, 553 (1970).

40. A. Johansson, P. Kollman, S. Rothenberg, Theor. Chim. Acta **29**, 167 (1973).

41. S. Fraga, Computer Physics Communications (in press).

42. R.S. Keynes, Sci. Am. 103, 126 (1979).

43. J.B. Chappel and A.R. Gofts, Biochem. J. 95, 393 (1965).

44. E.J. Harris and B.C. Pressman, Nature (London) 216, 918 (1967).

45. P. Mueller and D.O. Rudin, Biochem. Biophys. Res. Commun. 26, 398 (1967).

46. S.B. Hladky and D.A. Haydon, Biochim. Biophys. Acta 274, 294 (1972).

47. D.C. Tosteson, T.E. Andreoli, M. Tieffenberg and P. Cook, J. Gen. Physiol. 51, 373S (1968).

48. W.R. Veatch, R. Mathies, M. Eisenberg and L. Stryer, J. Mol. Biol. 99, 75 (1975).

49. W.R. Veatch and L. Stryer, J. Mol. Biol. 113, 89 (1977).

50. D.W. Urry, M.C. Goodall, J.D. Glickson and D.F. Mayers, Proc. Nat'l. Acad. Sci. U.S.A. 68, 1907 (1971).

51. E. Bamberg and K. Janko, Biochim. Biophys. Acta 465, 486 (1977).

52. R. Sarges and B. Witkop, J. Am. Chem. Soc. 87, 2011 (1965).

53. D.W. Urry, Proc. Nat'l. Acad. Sci. U.S.A. 68, 672 (1971).

54. R.J. Bradley, D.W. Urry, K. Okamoto and R. Rapaka, Science 200, 435 (1978).

55. W.R. Veatch, E.T. Fossel and E.R. Blout, Biochemistry
    13, 5249 (1974).

56. W.R. Veatch and E.R. Blout, Biochemistry 13, 5257
    (1974).

57. S. Weinstein, B.A. Wallace, E.R. Blout, J.S. Morrow and
    W. Veatch, Proc. Nat'l. Acad. Sci. U.S.A. 76, 4230
    (1979).

58. D.W. Urry, C.M. Venkatachalam, K.U. Prasad,
    R.J. Bradley, G. Parenti-castelli and G. Lenaz, Int. J.
    Quantum Chem. Quantum Biol. Symp. 8, 385 (1981).

59. M. Jean Browman, Lucy M. Carruthers, Karen L. Kashuba,
    Frank A. Momany, Marcia S. Pottle, Susan P. Rosen,
    Shirley M. Rumsey, QCPE (Prog. no. 286) (1975).

60. B. Maigret and B. Pullman, Theoret. Chim. Acta 35, 113
    (1974).

61. B. Maigret, D. Perahia and B. Pullman, Biopolymers 10,
    491 (1971).

62. E.T. Hesselnik and H.A. Scheraga, Macromolecules 5, 455
    (1972).

63. D.W. Urry, T.L. Trapane and K.U. Prasad, Int. J.
    Quantum Chem. Quantum Biol. Symp. 9, 31 (1982).

64. R. Koeppe, K. Hodgson and L. Stryer, J. Mol. Biol. 121,
    41 (1978).

65. V.B. Myers and D.A. Haydon, Biochim. Biophys. Acta 274,
    313 (1972).

66. D.W. Urry "Conformation of Biological Molecules and Polymers", Jerusalem Symposia on Quantum Chemistry and Biochemistry, Vol V, (Israel Academy of Sciences, Jerusalem) p.723 (1973).

67. D.W. Urry, C.M. Venkatachalam, A. Spisni, P. Läuger and M.A. Khaled, Proc. Nat'l. Acad. Sci. U.S.A. 77, 2028 (1980).

68. D.W. Urry, C.M. Venkatachalam, A. Spisni, R.J. Bradley, T.L. Trapane and K.U. Prasad, J. Membr. Biol. 55, 29 (1980).

69. C.M. Venkatachalam and D.W. Urry, J. Magn. Res. 41, 313 (1980).

70. Inger Nahringbauer, Acta. Cryst. B34, 315 (1978).

71. D.W. Urry, A. Spisni, M.A. Khaled, M.M. Long and L. Masotti, Int. J. Quantum Chem., Quantum Biol. Symp., 6, 289 (1979).

72. A. Finkelstein, "Drugs and Transport Processes", Ed. B.A. Canningham, Macmillan, p.241 (1974).

73. R.E. Koeppe II, J.M. Berg, K.O. Hodgson and L. Stryer, Nature (London) 279 723 (1979).

74. B. Hille, Biophys. J. 22, 283 (1978).

75. A.M. Sapse and A. Santoro, J. Comp. Chem. 2, 363 (1981).

76. A. Furusaki, the late Y. Tomiie and I. Nitta, Bull. Chem. Soc. Jap. 43, 3332 (1970).

77. C.R.C. Handbook of Chemistry & Physics, 60th Edition,

CRC Press (1979-1980).

78. D. André, R. Fourme and K. Zechmeister, Acta Cryst.,

B28, 2389 (1972).

79. V. Renugopalakrishnan and D.W. Urry, Biophys. J. 24 729

(1978).

80. E. Clementi, G. Corongiu and F. Lelj, J. Chem. Phys.

70, 3726 (1979).

81. J.M. Ritchie and H.P. Rang, Proc. Nat'l Acad. Sci. 80,

2803 (1983).

82. P. Hobza and R. Zahradnik "Weak Intermolecular

Interactions in Chemistry and Biology", Elsevier

Scientific Publishing Company (1980).

83. G.C. Lie and E. Clementi, J. Chem. Phys. 62, 2195

(1975).